A New Calculation Method for Life-Cycle Settlement of Soft Ground with Creep Treated by Columns

by

Pei-Chen Wu

Department of Civil and Environmental Engineering

The Hong Kong Polytechnic University, Hong Kong, China

Email: peichen.wu@connect.polyu.hk

Wei-Qiang Feng

Department of Ocean Science and Engineering

Southern University of Science and Technology, Shenzhen, China

Southern Marine Science and Engineering Guangdong Laboratory (Guangzhou), Guangzhou, China.

Email: fengwq@sustech.edu.cn

Jie-Qiong Qin

School of Civil Engineering

North China Univ. of Technology (NCUT), Beijing, China

Email: jq.qin@outlook.com

Kai-Fu Liu

School of Civil Engineering and Architecture

Zhejiang Sci-Tech Univ., Hangzhou 310018, China

Email: liukaifu@zstu.edu.cn

Jian-Hua Yin

Department of Civil and Environmental Engineering

The Hong Kong Polytechnic University, Hong Kong, China

Email: cejhyin@polyu.edu.hk

Abstract

For soft soils, the creep settlement plays an important role in the full life-cycle performance of infrastructures, which is a serious concern for engineers and researchers. Columns, *e.g.* deep cement mixed (DCM) soil columns, are commonly adopted to treat soft grounds in order to reduce the full-life settlement of the infrastructures. However, the creep behavior of soft grounds treated by DCM soil columns is often neglected, inducing underestimated total settlements or unexpected differential settlements. In this study, a new calculation method is developed for the life-cycle settlement of column-improved soft grounds by considering the creep of soft soils and load transfer between the columns and surrounding soils. A physical model test with double-layer soils improved by DCM soil columns was designed and performed to demonstrate the feasibility of the calculation method. It is found that the settlements calculated by the proposed method show good agreement with the measured data in the physical model. A parametric study was conducted, revealing that the calculated settlement of the double-layer soil improved by DCM columns can be largely influenced by the stress concentration ratio, the permeability of the DCM columns, and the area replacement ratio. Finally, the proposed method was applied to calculate the settlement in a real project.

Keywords: Consolidation settlement, calculation method, creep, DCM soil columns, physical model test

1. Introduction

The problem of excessive settlements occurs commonly in soft soils because of their large compressibility, high plasticity, and significant creep settlement. The time-dependent behavior of soft soils, such as the creep, has attracted the attention of many scholars (Adachi, 1982; Bjerrum, 1967; Garlanger, 1972; Mesri *et al.*, 1981; Zaman, *et al.*, 1991; Yin, 2015). In order to improve the performance of soft grounds, columns such as stone columns and deep cement mixed (DCM) soil columns, can be used to prevent excessive settlements (Baumann and Bauer, 1974; Shabu *et al.*, 2000; Han and Ye, 2001; Huang and Han, 2009; Chai *et al.*, 2015). However, creep settlements are usually neglected in the column-improved soft grounds.

Yin and Fang (2006, 2010), Fang and Yin (2007), Horpibulsuk *et al.* (2012), and Wu *et al.* (2019) conducted a series of physical model tests to investigate the dissipation of excess pore pressure, the failure mode of DCM soil columns, and stress transfer on marine clay improved by DCM soil columns. Balaam and Booker (1981) presented an analytical solution based on the elasticity theory for predicting settlements of soil reinforced by granular columns under a rigid loading. Zhao *et al*. (2017) proposed a simplified axisymmetric model with a deformed shape function to simulate the deformation and arching effect of column-supported embankment systems. Han and Ye (2001) proposed a simplified method to calculate the consolidation rate of foundations reinforced by stone columns. Later, smear and well resistance effects were considered by Han and Ye (2002). Chai *et al.* (2010) proposed a method for calculating consolidation settlements of soft soil improved by floating columns based on the consolidation theory of double-layer soils. Zhou *et al*. (2017) developed analytical solutions to the axisymmetric consolidation of a multi-layer soil system under surcharge combined with vacuum preloading. Chen *et al*. (2008) and Zhou *et al*. (2021) proposed theoretical methods for studying settlements and load transfer mechanisms of column-supported embankments with the consideration of penetration of column toe and column-soil interaction. The abovementioned methods pertain to primary consolidation only and ignore the creep behavior of the soft soil. Madhav *et al.* (2010) presented a simple method to calculate the creep or "secondary" consolidation settlement of soft soils improved by granular piles. However, this method only considers the creep settlement after the consolidation stage. In addition, this method relies on a tedious iterative process to calculate settlement, which is not suitable for practical projects. Sexton et al. (2017) and Wu *et al.* (2020) found that the creep behavior of soft soil still affects the long-term settlements and load transfer even though the creep behavior is reduced by the columns. However, there is a lack of calculation methods to predict the life-cycle settlements of soft soils improved by columns considering the creep of the soft soils.

In this study, an easy-to-use method, developed from the new simplified method (Feng and Yin, 2017; Feng *et al.,* 2020a; Chen *et al.,* 2021), is derived and developed to calculate the life-cycle settlement of the soft soil improved by columns. In particular, the influences of the creep behavior of the improved soft ground are analyzed. Afterward, the proposed method is verified by a physical model including a double-layer soft soil with the floating DCM soil columns. In addition, it is demonstrated that this method can be also applied to soft soils treated by prefabricated vertical drains (PVDs) considering PVDs as special columns. Furthermore, this calculation is utilized in the Pacific Highway Upgrade embankment project in Australia to illustrate its feasibility.

2. Derivation of a Simple Calculation Method for Life-Cycle Settlements of Soft Grounds Improved by Columns

2.1 Review of the new simplified Hypothesis B method

In practical applications, simple methods are appreciated for engineers to make acceptable predictions. For estimating consolidation settlements of soft soils exhibiting creep, there are mainly two types of methods. One is based on Hypothesis A, in which no creep compression occurs during the "primary" consolidation period. The other is based on Hypothesis B, in which creep compression occurs in both "primary" and "secondary" consolidation. Hypothesis A method is normally utilized to calculate the consolidation settlements for soft grounds by geotechnical engineers due to its simplicity (Shepheard and Williamson, 2018). Although Hypothesis A method is easy to utilize, there are some contradictions with the axioms of continuum mechanics (Degago *et al.,* 2013). Yin and Graham (1989, 1994, 1996) proposed an elastic visco-plastic (EVP) constitutive model to describe the time-dependent behavior of soft soils. By coupling the consolidation analysis and the EVP constitutive model, a rigorous Hypothesis B method was presented for long-term settlement calculation of soft soils (Yin and Zhu, 1999; Zhu and Yin, 2000; Zhu *et al.,* 2001; Yin and Zhu, 2020). However, it involves a set of nonlinear partial differential equations which need to be solved by numerical methods.

Based on the concept of equivalent time (Bjerrum, 1967; Yin and Graham, 1994), Yin and Feng (2017) proposed a new simplified method to calculate the consolidation settlement of soft soils with creep. In this method, the complicated nonlinear partial differential equations coupling 1D elastic visco-plastic (EVP) constitutive model and consolidation were simplified as:

$$S_{total} = U_a S_f + S_{creep} \tag{1}$$

$$S_{creep} = \alpha S_{creep,f} + (1-\alpha) S_{secondary} \tag{2}$$

where $U_a S_f$ is the settlement during "primary" consolidation, U_a is the average degree of consolidation, $S_{creep,f}$ is the creep settlement under the final effective stress ignoring the excess pore pressure coupling, $S_{secondary}$ is the secondary consolidation settlement, α is a parameter to describe the coupling of consolidation and creep, it is suggested to take α =0.8. The average degree of consolidation, U_a, can be calculated by Terzaghi 1D consolidation theory for one single soil layer. Later, this method was improved to be capable of calculating the settlements of double-layer soils and the soils with vertical drains by revising the average degree of consolidation (Feng and Yin, 2017, 2018). For the reclamations and embankments on soft soils, ramp loading is more reasonable than constant loading. Therefore, Feng *et al.* (2020a) updated the new simplified method to calculate the settlements of multi-layer soils with creep under multi-stage ramp loading. Besides, $S_{creep,d}$ (delayed creep settlement with respect to the final effective stress under the given loading due to the excess pore pressure coupling) is used to replace the "secondary" settlement term in Eq. (2), as presented in Eq. (3):

$$S_{creep} = \alpha S_{creep,f} + (1-\alpha) S_{creep,d} \tag{3}$$

where $S_{creep,d}$ is only taken into account when $U_a = 98\%$ is reached in the field, α is a parameter combining the final creep settlement and delayed creep settlement. And $\alpha = U_a$ is used instead of 0.8.

When no vertical drains are involved, the consolidation of the soft soil is treated as 1D consolidation. The average degree of consolidation follows the approximate formulas of Terzaghi's solution for 1D condition, expressed as:

$$U_v = \begin{cases} \left(\dfrac{4T_v}{\pi}\right)^{0.5} & \text{for } U_v \le 0.6 \\ 1-10^{\frac{-T_v+0.085}{0.933}} & \text{for } U_v > 0.6 \end{cases} \tag{4}$$

$$T_v = \frac{c_v t}{H^2} \tag{5}$$

where T_v is the time factor, c_v is the coefficient of consolidation. When vertical drains are involved, radial consolidation must be considered (Barron, 1947; Hansbo, 1979; Long and Covo, 1994; Lu *et al.*, 2019). The average degree of consolidation is calculated as:

$$U_a = 1-\left(1-U_v\right)\left(1-U_r\right) \tag{6}$$

For the cases of soils under ramp loading, Zhu and Yin (2004) method can be adopted to determine the average degree of consolidation.

However, the simplified method reviewed above is only suitable for soft soils without column reinforcement. In the case of soft soils improved by columns, the stress distribution is influenced by the columns due to which the simplified method above is no longer capable of calculating the settlements. With regard to the wide existence of column-improved soft ground, it is necessary to develop a simple calculation method for the soft soil layers improved by columns in practice.

2.2 The simple calculation method for life-cycle settlement of soft ground improved by columns

To develop a simple method for calculating the life-cycle settlements of soft soils improved by DCM soil columns, four assumptions are introduced:

(1). The deformations of the columns and the surrounding soils are under equal strain condition.

(2). The lateral deformations of the columns and the surrounding soils are ignored.

(3). The columns are considered as elastic materials.

(4). The creep coefficient of the soil is a constant.

Normally, columns are arranged in a square pattern or triangular pattern. In this study, the square pattern is taken as an example to analyze a unit cell. For the square pattern, $r_e = d_e / 2 = 1.13 s_c / 2$. For the triangular pattern, $r_e = d_e / 2 = 1.05 s_c / 2$, where s_c is the center-to-center spacing of the columns. Owing to the load transfer between the columns and surrounding soils, there is an unloading process of total vertical stress on the surrounding soils (Madhav *et al.*, 2010; Wu *et al.,* 2020).

Figure 1 shows the schematic diagram of the unit cell for column-improved soft ground with the typical loading distributions between the column and soils. According to force equilibrium in the vertical direction, the relationship between the vertical stresses on the column and the surrounding soil is expressed as:

$$\sigma_s A_s + \sigma_c A_c = pA \tag{7}$$

where A_c is the area of the column, and A_s is the area of the surrounding soil, $A = A_c + A_s$.

Considering $\sigma_c = n_s \sigma_s$, Eq. (7) can be rewritten as:

$$\sigma_s = \frac{p}{1 - A_r + n_s A_r} \tag{8}$$

where n_s is the stress concentration ratio which is related to the stiffness difference between the soil and column as well as area replacement ratio, which can refer to Han and Ye (2002),

$A_r = \left(r_c / r_e\right)^2$ is the area replacement ratio of the column-improved soft soil. r_e is the radius of zone influenced by the columns, r_c is the radius of the columns.

If there is no excess pore water pressure, the stress-strain state of the surrounding soil would go along the path of *Point 0* to *Point a* to *Point b* in Figure 2. However, the unloading process induces a rebounded deformation of surrounding soils, which violates the equal strain assumption. Given that the loading on the column increases monotonically before the column yields, there should be no rebounding on the column. In fact, at the beginning of the consolidation, most of the loading is taken by the pore water in surrounding soils, which induces that the effective stress is assumed to follow the red dash line in Figure 2. *Point 1* is corresponding to the state where the consolidation of the soft ground is completed. σ_s' is the effective vertical stress acting on the top of the surrounding soils.

The soft soil layer is divided into several sublayers (1, 2, 3, …, *m*, …). The vertical stress acting on the sublayer *m* is $\sigma_{v0,m}' + \sigma_s' = \sigma_{v1,m}'$, $\sigma_{v0,m}'$ is the initial effective stress at the mid-depth of the sublayer *m*. The final strain of the sublayer *m* without creep is calculated as:

$$\varepsilon_{f,m} = \frac{C_s}{v}\log\left(\frac{\sigma_{v1,m}'}{\sigma_{v0,m}'}\right) \qquad \text{for } O.C. \tag{9}$$

$$\varepsilon_{f,m} = \frac{C_s}{v}\log\left(\frac{\sigma_{vp1,m}'}{\sigma_{v0,m}'}\right) + \frac{C_c}{v}\log\left(\frac{\sigma_{v1,m}'}{\sigma_{vp1,m}'}\right) \qquad \text{for } N.C. \tag{10}$$

where C_s and C_c are the swelling index and the compression index of the soil, which can be obtained from oedometer tests with $t_0 = 1$ day. v is the specific volume. $\sigma_{vp1,m}'$ is the pre-consolidation pressure, as shown in Figure 3. *O.C.* stands for over-consolidated soils. *N.C* denotes normally consolidated soils. The effect of area replacement ratio is considered by Eq (8). If there is no column, $A_r = 0$, $\sigma_s' = p$, then Eqs. (9) and (10) become those used in the simplified Hypothesis B method proposed by Feng *et al*. (2020a).

The total final consolidation settlement of the soft soil is the sum of that of each sublayer:

$$S_f = \sum_{m=1}^{n} \varepsilon_{f,m} H_m \tag{11}$$

where H_m is the thickness of the sublayer *m*.

Considering the function of the columns on controlling creep behavior of the surrounding soil, creep strains are calculated by the following equations:

$$\varepsilon_{creep,f,m} = \left(1 - A_r\right)^{\beta} \frac{C_{\alpha e}}{v} \log\left(\frac{t_o + t_{e,m}}{t_o + \Delta t_{e1,m}}\right) \quad \text{for } O.C. \tag{12}$$

$$\varepsilon_{creep,f,m} = \left(1 - A_r\right)^{\beta} \frac{C_{\alpha e}}{v} \log\left(\frac{t_o + t_e}{t_o}\right) \quad \text{for } N.C. \tag{13}$$

$$\varepsilon_{creep,d,m} = \left(1 - A_r\right)^{\beta} \frac{C_{\alpha e}}{v} \log\left(\frac{t_o + t_{e,m}}{\Delta t_{e,m} + t_{EOP,field}}\right) \quad \text{for } O.C. \tag{14}$$

$$\varepsilon_{creep,d,m} = \left(1 - A_r\right)^{\beta} \frac{C_{\alpha e}}{v} \log\left(\frac{t_o + t_e}{t_{EOP,field}}\right) \quad \text{for } N.C. \tag{15}$$

where $C_{\alpha e}$ is the creep coefficient of the soft soil, which can be obtained from oedometer tests corresponding $t_0 = 1$ day. It should be noted that the interaction between the columns and surrounding soils due to the interfacial friction could change the stress state of the soils and hence reduce the creep settlement. However, introducing this interaction would complicate the settlement calculation procedure. Here, a reduction factor β related to stress decrement of the surrounding soils and their stress state is adopted to simply evaluate the influence of the interaction between the columns and the soils. $\beta = 2.2\sin\left(\varphi_c\right)$ was proposed by Feng *et al.* (2020b) for soft grounds improved by stone columns or sand compaction piles (φ_c is the friction angle of stone or sand materials). In this study, $\beta = 1$ is used for DCM soil columns. $\Delta t_{e,m}$ and $t_{e,m}$ are the calculated equivalent time and can be determined from the following equations:

$$\Delta t_{e,m} = t_o \times 10^{\left(\left(\varepsilon_{f,m}-\varepsilon_{vp,m}\right)\frac{v}{C_{\alpha e}}\right)} \left(\frac{\sigma'_{v0,m}+\Delta\sigma'_{v,m}}{\sigma'_{vp,m}}\right)^{-\frac{C_c}{C_{\alpha e}}} - t_o \tag{16}$$

$$t_{e,m} = t - t_o + \Delta t_{e,m} \quad \text{for } O.C. \tag{17}$$

$$t_e = t - t_o \quad \text{for } N.C. \tag{18}$$

where $t_{EOP,field}$ is the time when $U_a = 98\%$ in the field.

Then, the creep settlement can be obtained by substituting Eqs. (19) and (20) into Eq. (3).

$$S_{creep,f} = \sum_{m=1}^{n} S_{creep,f,m} = \sum_{m=1}^{n} \varepsilon_{creep,f,m} H_m \tag{19}$$

$$S_{creep,d} = \sum_{m=1}^{n} S_{creep,d,m} = \sum_{m=1}^{n} \varepsilon_{creep,d,m} H_m \tag{20}$$

With regard to the calculation of the degree of consolidation of column-improved ground, the smear effect is considered in the average degree of consolidation by using Han and Ye (2001) method:

$$U_r(t) = 1 - e^{-\frac{8}{F}T_{rm}} \tag{21}$$

where $T_{rm} = \dfrac{c_{rm} t}{d_e^2}$ is the modified time factor, which considers both effects of the drainage and stress reduction, c_{rm} is the modified coefficient of consolidation, F is the parameter, expressed as:

$$\begin{aligned} F = {} & \frac{N^2}{N^2-1}\left(\ln\frac{\sqrt{1/A_r}}{S} + \frac{k_r}{k_s}\ln S - \frac{3}{4}\right) + \frac{A_r S^2}{1-A_r}\left(1-\frac{k_r}{k_s}\right)\left(1-\frac{A_r S^2}{4}\right) \\ & + \frac{k_r}{k_s}\frac{A_r}{1-A_r}\left(1-\frac{A_r}{4}\right) + \frac{32}{\pi^2}\frac{k_r}{k_c}\left(\frac{H}{d_c}\right)^2 \end{aligned} \tag{22}$$

$$c_{rm} = c_r\left(1 + \frac{n_s A_r}{1-A_r}\right) \tag{23}$$

where $S = \frac{r_s}{r_c}$, r_s is the radius of smear zone, d_e is the diameter of zone influenced by the columns, d_c is the diameter of the columns, k_r is the radial coefficient of permeability of the surrounding soil, k_s is the radial coefficient of permeability of the soil in smear zone, k_c is the coefficient of permeability of the columns, and c_r is the radial coefficient of consolidation. The average degree of consolidation is calculated by Eq. (6). A spectral method proposed by Walker and Indraratna (2009) and Walker *et al*. (2009) can be used to solve the consolidation problem and estimate the average degree of consolidation of a multi-layer soil.

Figure 3 presents a schematic diagram of stress-strain paths in a double-layer soft soil under two-staged loading. The PVD can be regarded as a special column with only geometrical and hydraulic functions but no mechanical assistance to the soft soil. The proposed simple method can be directly used to calculate the settlements of PVD-improved soft soils by using $\boldsymbol{n}_s = \mathbf{1}$ in Eq. (22). Figure 4 presents the calculation flow chart of the simple method.

The average vertical stress $\sigma_{c,b}$ acting on the bottom of the columns can be estimated by:

$$\sigma_{c,b}A_c = \sigma_c A_c + 2r_c \pi L \overline{\tau} \tag{24}$$

where L is the length of the column. $\overline{\tau}$ is the average interfacial friction between the column and the surrounding soil. The average vertical stress $\sigma_{s,b}$ on the surrounding soil at the same level as the bottom of the columns can be calculated by:

$$\sigma_{c,b}A_c + \sigma_{s,b}A_s = pA \tag{25}$$

The average interfacial friction can be estimated by:

$$\overline{\tau} = \mu_f K_0 \left(\frac{\sigma_s + \sigma_{s,b}}{2} \right) \tag{26}$$

K_0 is the at-rest earth pressure coefficient, μ_f is the interfacial friction coefficient. Therefore, Eq. (24) can be rewritten as:

$$\sigma_{s,b}A_c = \sigma_s A_c + 2r_c \pi L \mu_f K_0 \left(\frac{\sigma_s + \sigma_{s,b}}{2} \right) \tag{27}$$

The average vertical stresses $\sigma_{c,b}$ and $\sigma_{s,b}$ can be solved from Eqs. (25) and (27).

3. Experiment Setup

3.1 Test Materials

The soft soil used in this study is Hong Kong marine deposits (HKMD), which were excavated from a coastal area near Lantau Island. The basic properties of the reconstituted HKMD are listed in Table 1. Details on the HKMD can be referred to Yin and Feng (2017). The DCM soil columns were made by mixing the HKMD with the initial water content of 100% and ordinary Portland cement at a cement/soil ratio (dry mass of cement to dry mass of soil) of 20%. The basic properties of the DCM soil columns are listed in Table 2.

A new type of PVD (New Colbonddrain CX1000) was used in this study. Different from the conventional PVDs with separate fleece (or sleeve) and core, the new PVD, which is based on an innovative extrusion and shaping technique, integrates fleece and core. Identical to the conventional PVDs, the new PVDs are 100 mm in width and 4 mm in thickness. The PVDs were cut into 30 mm in width and then inserted when the soil was in the slurry state so that the smear zone can be ignored in the loading stages.

3.2 Model preparation and transducers

The experiment was conducted in a physical box with two stainless steel walls and two transparent acrylic plates (900mm× 300mm× 870mm), which was introduced in Yin and Fang (2010) and Qin *et al.* (2020). Two frames were used to apply the horizontal restriction to the acrylic plates. A double-layer soft soil was then prepared. 12 PVDs and 12 DCM soil columns in a square pattern with a spacing of 150 mm were used separately to improve the soft soil at different stages, as shown in Figure 5, respectively. A porous aluminum plate was placed on the soft soil for two linear variable differential transformers (LVDTs) to measure the total settlements. Similar to Wu *et al.* (2019) and Ho *et al.* (2020), the DCM soil columns were prepared following the way of casting concrete specimens to ensure the quality of the columns. After curing of 28 days, the 12 DCM soil columns were installed into the upper layer of the soft soil. The gaps between columns and surrounding soil were filled by cement-soil HKMD slurry.

The layout of transducers in the physical model is shown in Figure 5. Two pore pressure transducers (PPT1 and PPT2) were installed at the bottom of the lower soil layer and two pore pressure transducers (PPT3 and PPT4) were placed at the interface of the upper layer and lower layer to monitor the dissipation of excess porewater pressure. Two earth pressure cells (EPC1 and EPC2) were installed on the top of two DCM soil columns, two earth pressure cells (EPC3 and EPC4) were installed at the bottom of the columns, and another two earth pressure cells (EPC5 and EPC6) were placed on the top of the upper layer, which were in the middle between columns. Two LVDTs (LVDT1 and LVDT2) were placed at the right and left edges of the plate on the top of the soft soil layer.

3.3 Load procedures in the test

First of all, a soft soil layer with 474 mm was prepared under a loading of 15 kPa. After the settlement of the soft soil layer was stable, the double-layer soft soil was then prepared on the previous soil layer by pouring a layer of HKMD slurry. Pre-consolidation pressure of 5 kPa was applied on the top of the upper layer of the soil after installing PVDs. The lower layer of the soft soil was 324 mm and the upper layer was 382 mm after the pre-consolidation. A loading of 12 kPa was applied to the double-layered soft soil (Stage I) for 53 days followed by an unloading process (Stage II). In Stage I, the upper layer was normally consolidated while the lower layer was over-consolidated with pre-consolidation loading of 15 kPa. In Stage II, the loading was unloaded from 12 kPa to 4 kPa, and the loading of 4 kPa was maintained on the soft soil for 30 days. The measured settlement of the double-layer soft soil going through a loading and unloading process is plotted in Figure 6. In Stage III, the PVDs in the upper layer were replaced by DCM soil columns. Due to the load transfer between DCM soil columns and the surrounding soil in the upper layer, the surrounding soil in the upper layer turned over-consolidated. The upper layer of the soft soil was trimmed to 300 mm in order to have the same height as the length of the columns. The lower layer was 310 mm before applying a double-staged loading (from 11 kPa to 20 kPa). During the test, the vertical stresses on the top of DCM soil columns, the vertical stresses on the top of the surrounding soil, and the vertical stresses beneath the DCM soil columns were measured.

4. Experiment Results

Figure 7 shows the variation of average vertical stresses on the columns and the surrounding soils measured by EPCs. The value of the vertical stress on the top of the DCM soil columns is the average value of the measured data from EPC1 and EPC2, while that on the top of the soft soil is the average value of the measured data from EPC5 and EPC6. When a loading of 11 kPa was applied, the vertical stress on the DCM soil columns (27.83 kPa) is higher than the applied loading. Although there was no significant unloading process on the soft soil, the vertical stress on the soft soil (8.46 kPa) is lower than the applied loading, which demonstrates that the applied loading concentrates on the DCM soil columns with the *n* value of 3.29.

The vertical stresses acting on the top of the lower soft soil where beneath the DCM soil columns were measured by EPC3 and EPC4, and the average value of the measured stresses was 12.47 kPa, which was larger than the applied loading 11 kPa. According to the area replacement ratio, the stress on the top of the lower soft soil where between the columns was 10.90 kPa, which was almost identical to the applied loading. It seems that the stress distribution on the top of the lower layer was nearly uniform in this study. It should be noted that the penetration of the columns (less than 10 mm in this study) was not considered in the proposed method for settlement calculation but can be estimated using the simple equations proposed by Pongsivasathit et al. (2013) and Liu (2022) with correction. Theoretical equations proposed by Chen et al. (2008) and Zhou et al. (2021) can be also used to consider both penetration of columns and column-soil interaction. However, the equations need to be solved using numerical approaches, which are not easy for practical use by engineers.

There is a noticeable unloading process on the top layer of the soft soil when the applied loading is increased to 20 kPa. As the consolidation occurs, the unloading process is slowed down, and the average vertical stress on the soft soil is approaching a stable value of 8.57 kPa. While that of the DCM soil columns mainly increases with time and then approaches 81.42 kPa so that the stress concentration ratio is 9.50. Meanwhile, the average vertical stresses on the bottom of the columns measured by EPC3 and EPC4 are nearly stable at 20 kPa, which is the applied loading. This uniform stress distribution is used in the following section for the settlement calculation.

Figure 8 shows that the excess pore pressure in the upper layer dissipates faster than the one in the lower layer. It is because of the shorter drainage path in the upper layer and the effect of the DCM soil columns on improving the coefficient of consolidation. The calculated excess pore pressures are based on the calculated average degree of consolidation and the loading on the soft soil. Based on the pore pressure and vertical stress, the average degree of consolidation U_a in the upper layer and the stress concentration ratio n_s on the top of the upper layer are plotted *versus* time in Figure 9. It can be seen that the curve of U_a has a similar trend to that of n_s.

5. Verification of the Simple Calculation Method

The proposed simple method is verified by the physical model test in Stage III. The details of the consideration of multi-layer soils under multi-staged loading can refer to Feng *et al.* (2020a).

The vertical permeabilities used for the settlement calculation are determined based on the results of an oedometer test by the void ratios of the soil layers with respect to different loadings. The horizontal permeabilities are calculated by multiplying 2 to the vertical permeability according to the historical data of the HKMD (Zhu *et al.*, 2001).

5.1 Double-layer soft soil treated by DCM soil columns

Smear zone is considered in the case with DCM soil columns, the radius of the smear zone is 32 mm. The value of the permeability of the soil in the smear zone depends on soil types, column types, and the installation methods of different columns. For HKMD treated by PVDs, the ratio of the permeability of the soft soil in the smear zone to that in the uninfluenced zone (k_s/k_r) ranges from 0.4 to 1 (Feng and Yin, 2018; Yin *et al*., 2022; Yu *et al*., 2007). However, the reduction in permeability of the soft soil in the smear zone due to the installation of DCM soil columns is not exactly known. In this study, k_s/k_r = 0.8 was selected for HKMD treated by DCM soil columns. But the influence of k_s/k_r on the calculated settlement is negligible. Based on the measured data, the lower layer of the soft soil can be treated as an over-consolidated soft soil subjected to a uniform loading, and its settlement can be calculated by the proposed simple method by using $A_r = 0$. While the settlement of the upper layer is calculated by the simple method using $A_r = \left(r_c / r_e\right)^2$.

Figure 3 demonstrates the stress-strain paths during Stage III. When applying the first loading, the effective vertical stress on the upper layer of the soft soil moves from *Point 0* to *Point 1*, followed by a creep from *Point 1* to *Point 1'*. When applying the second loading, the effective vertical stress on the upper layer of the soil soils moves from *Point 1'* to *Point 2*, followed by a creep from *Point 2* to *Point 2'*.

It should be noted that the effective vertical stresses acting on the upper layer of the soft soil need to be calculated by considering the load transfer between the DCM soil columns and the surrounding soil. According to the measured data, the stress concentration ratios at *Point 1* and *Point 2* are around 3.29 for the 11 kPa loading and 9.50 for the 20 kPa loading, respectively. Therefore, the effective vertical stresses at *Point 1* and *Point 2* are calculated by Eq. (11) with $n_s = 3.29$ and $n_s = 9.50$.

Table 5 presents the results of stresses and strains as a reference. An example of calculation details is attached in the Appendix. The measured settlement of the double-layer soft soil with

DCM soil columns and calculated settlement from the simple method are compared in Figure 10.

5.2 Double-layer soft soil treated by PVDs (Stage I and II)

In Stage I with the applied loading of 12 kPa, the upper layer of the soft soil was normally consolidated, while the lower layer of the soft soil was over-consolidated with the pre-consolidation pressure of 15 kPa. In Stage II, both top and bottom layers were over-consolidated when the 12 kPa was unloaded to 4 kPa.

Here, the PVD-improved soft soil is treated as a special case of the column-improved soft soil without mechanical contribution (loading transfer), corresponding to $n_s = 1$ in Eq. (11). The radius of columns is replaced by the equivalent radius of the PVDs. Long and Covo (1994) method is adopted to calculate the equivalent radius of the PVDs. In addition, the PVDs were installed into the soft soil when the soil was in a state of slurry, therefore, the smear effect is not considered in the calculation. Well resistance is also ignored in Stage I and Stage II.

Figure 6 shows the settlement result calculated by the proposed simple method and the measured settlement in Stage I and Stage II. It can be seen that the simple method under-estimates the settlement at the beginning but gives a close result to the measured settlement after 30 days. In Stage II, the calculated settlement shows good agreement with the measured data. The calculation procedure is also listed in Table 6 as a reference. An example of calculation details is attached in the Appendix.

5.3 Parametric analysis

(a) Stress concentration ratio

Figure 11 shows the calculated results from the simple method using different stress concentration ratios. For the first loading, the calculated settlement decreases with increasing the value of the stress concentration ratio. For the second loading, a similar relationship can be found between the calculated settlement and the stress concentration ratio. For the same area replacement ratio, the larger the stress concentration ratio, the higher stiffness of the DCM soil columns relative to the surrounding soils, which means the stiffer columns can control the settlements more effectively.

(b) Coefficient of permeability

The coefficient of permeability of the DCM soil columns is varied to investigate their influence on settlement calculation. The settlement results with different values of the coefficient of permeability are plotted in Figure 12. It is shown that the larger value of the coefficient of permeability of the DCM soil column can accelerate the consolidation process.

(c) Area replacement ratio

In order to investigate the influence of area replacement ratio on settlement calculation, different values of the diameter of the DCM soil columns are analyzed correspondingly. Figure 13 shows the calculated settlements from the simple method using different area replacement ratios. As expected, the long-term settlement decreases with increasing the area replacement ratio. At the beginning of the primary consolidation, the calculated settlement using a larger value of area replacement ratio is larger than that using a smaller area replacement ratio. This can be explained by the effect of the DCM soil columns on accelerating the consolidation process of the surrounding soils.

Following the strategy of studying the creep settlement of the stone column-treated soils by Sexton *et al.* (2016 and 2017), a so-called creep settlement improvement factor, n_{creep}, is defined as the ratio of $\mu^*_{untreated}$ and $\mu^*_{treated}$ to evaluate the function of the DCM soil columns in reducing the creep effect of soft soil. “Untreated” refers to $A_r = 0$, while “treated” is corresponding to $A_r > 0$. Figure 13 demonstrates the meaning of $\mu^*_{untreated}$ and $\mu^*_{treated}$. It should be noted that the creep behavior of the lower layer soft soil also contributes to the overall creep settlement in this study.

The relationship of n_{creep} and area replacement ratio A_r is plotted in Figure 14. The value of n_{creep} increases with increasing the area replacement ratio. But this value tends to be stable when the area replacement ratio approaches 30%, which means that increasing the diameter of the DCM soil columns would not further reduce the creep effect of the soil. Wu *et al.* (2020) also pointed out that the influence of DCM soil columns on the creep of the surrounding soils can be neglected if the area replacement ratio is larger than 30%. Nevertheless, the total settlements can be further reduced by increasing the area replacement ratio. Based on the results of n_{creep}, the authors recommend the range of the area replacement ratio for reference, which is 10% ~ 25%. Below the range, the assistance of the DCM soil columns in reducing the creep settlement is not significant. Choosing an area replacement ratio beyond the range would neither provide a significant reduction in creep settlement nor be economical for practical use.

Other factors, such as mechanical properties of the columns, stress states of the surrounding soils, and external loading conditions, can also influence the creep settlements (Sexton *et al.,* 2017; Sivakumar *et al.,* 2021; Wu *et al.,* 2020).

6. Application in a real project

6.1 Basic information

The embankment was constructed on a soft soil subsoil improved by DCM columns. DCM columns with a diameter of 0.8 m and a spacing of 1.3 m were installed in a square pattern beneath the crest for controlling settlements. DCM walls with a spacing of 3 m formed by columns were installed at the corner of the embankment for maintaining stability. The geometries of the embankment with the underlaid subsoil and the layout of DCM columns are shown in Figure 15. The top layer of the subsoil is firm clay (a depth of 0-0.5 m), underlaid by the soft clay layer (a depth of 0.5-8.5 m) below which is a layer of silty sand with a thickness of 5 m, a layer of firm clay with a thickness of 3.5 m, and a layer of stiff to hard clay with a thickness of 8 m. The detailed subsoil profile can be found in Yapage *et al.* (2014). The properties of materials are listed in Table 7. The relationship between the OCR of soft clay and depth is shown as follows:

$$OCR = \begin{cases} \left(\dfrac{7.5}{z}\right)^{0.51} & \left(0.5\ \mathrm{m} \le z \le 4.5\,\mathrm{m}\right) \\ 1.3 & \left(4.5\ \mathrm{m} \le z \le 8.5\,\mathrm{m}\right) \end{cases} \tag{28}$$

where z is the depth from the bottom of the embankment. It should be noted that creep behavior is taken into consideration in the soft clay layer. Creep coefficient is estimated by the equation given by Yin *et al.* (2010):

$$\eta_{L1} = C_\alpha \big/ \left(C_c - C_s\right) \tag{29}$$

where $C_\alpha = 2.3C_{\alpha e}$. The value of η_{L1} ranges from 2%~8.9%. In this study, $\eta_{L1} = 5\%$ is used.

A settlement plate was installed 9.8 m away from the center of the embankment to measure the settlement of subsoil, as shown in Figure 15(b).

6.2 Settlement calculation

Although there are five soil layers below the embankment, the soft clay layer contributes the most to the settlement on the top of the subsoil. The creep settlements of those layers beneath the soft clay layer are ignored. The top firm clay can be considered as a part of the soft clay layer but with OCR = 135 (Yapage *et al.*, 2014). In addition, the bottom boundary of the soft clay layer is perceived as impermeable, provided the permeabilities of the firm and stiff clay are around 100 times smaller than the permeability of the soft clay layer. The settlement calculation can be simplified as:

$$S = U_a S_f + \left[\alpha S_{creep,f} + \left(1-\alpha\right) S_{creep,d}\right] + U_v \sum \frac{\left(p + \sigma'_{vk}\right) H_k}{E_k} \tag{30}$$

where the last term in Eq. (26) is the settlement beneath the soft clay layer, E_k, σ'_{vk}, and H_k are Young's modulus, vertical effective stress, and thickness of sublayer *k* beneath the soft clay layer.

The embankment is converted to a ramp loading of 105.83 kPa with the construction time, $t_c = 40\text{ days}$, as shown in Figure 15(c). When applying the proposed simple method, the top firm clay is treated as sublayer 1, and the soft clay layer is divided into eight sublayers (sublayers 2~ 9).

Following the calculation procedure, as shown in Figure 4, the total settlement $S_{total}(t)$ can be calculated. To consider the ramp loading of the construction of the embankment, the term of consolidation settlement, $U_a S_f$, in Eq. (1) needs to be corrected into S_{corr} according to the correction method for the degree of consolidation proposed by Terzaghi (1943). Yin and Zhu (2020) presented a simple equation to calculate the corrected consolidation settlement:

$$S_{corr} = \begin{cases} U_a\left(\dfrac{t}{2}\right) S_f \dfrac{p(t)}{p(t_c)} & (t \le t_c) \\ U_a\left(t - \dfrac{t_c}{2}\right) S_f & (t > t_c) \end{cases} \tag{31}$$

where t_c is the construction time; $p(t)$, $U_a(t)$, and $s(t)$ are the embankment loading, the average degree of consolidation, and the settlement at t, respectively; S_f is the final consolidation settlement which can be determined by Eq. (11).

It should be noted that the stress concentration ratio n_s in Eq. (8) remains unknown. In order to determine n_s, it is necessary to take into account the soil arching developed in the embankment to calculate the vertical stresses taken by DCM columns and the surrounding soil. Adapted Terzaghi method proposed by Sloan *et al.* (2011) was used to consider the soil arching effect and calculate n_s.

Figure 16 presents the calculated settlement of the subsoil. The settlement calculated by the simple method shows good agreement with the measured data. A slight underestimation is mainly due to the ignorance of the lateral deformation of the subsoil. Nevertheless, the proposed simple method has illustrated its feasibility for settlement calculation.

7. Conclusions

In this paper, a simple method for calculating the settlement of soft soils exhibiting creep improved by DCM soil columns has been presented. With newly proposed equations for determining creep settlements, this method can consider the function of the columns in controlling the creep of improved soft soil grounds. A physical model test was built to investigate the settlements of double-layer soft soil improved by PVDs and DCM soil columns. The proposed method was verified by measured data from the physical model tests and applied to calculate the settlement of a real project. Findings and conclusions are drawn as follows:

(a) The calculated results of the simple method agree well with the experimental data of both the double-layer soft soil improved by DCM soil columns and that improved by PVDs.

(b) Stress concentration ratio is an important factor to influence the settlement results of the simple method. The calculated settlement decreases with increasing the stress concentration ratio.

(c) Based on the results of the parametric study, an area replacement ratio of 10%~25% is recommended. Below the range, the assistance of the DCM soil columns in reducing the creep settlement is not significant. Choosing an area replacement ratio beyond the range would neither provide a significant reduction in creep settlement nor be economical for practical use.

(d) The settlement calculated by the proposed method agrees well with the measured data of a real project reported by Yapage *et al.* (2011).

It should be noted that the proposed simple method has limitations in considering the penetration depth of columns and the actual interaction between columns and surrounding soils. If the penetration is significant and the column-soil interaction is the main concern, this method must be used with care with somewhat modification, which requires further study.

Conflict of interest

No potential conflict of interest was reported by the authors.

Data Availability Statement

All data that support the findings of this study are available from the corresponding author upon reasonable request.

Acknowledgements

We are thankful for the financial support given by the Key Special Project for Introduced Talents Team of Southern Marine Science and Engineering Guangdong Laboratory (Guangzhou) (GML2019ZD0210), Project from Shenzhen Science and Technology Innovation Commission (JCYJ20210324105210028), the grand of Southern Marine Science and Engineering Guangdong Laboratory (Guangzhou) (K19313901). The work in this paper is also supported by General Research Fund (GRF) (PolyU 152179/18E, PolyU 152130/19E, PolyU 15210020), a Research Impact Fund (R5037-18), and a Theme-based Research Scheme project T22-502/18-R from Research Grants Council of Hong Kong Special Administrative Region Government of China. The work is also supported by grants (CD82 and CD7A) from the Research Institute of Land and Space, The Hong Kong Polytechnic University, China.

References

Adachi, T., & Oka, F. (1982). Constitutive equations for normally consolidated clay based on elasto-viscoplasticity. Soils and foundations, 22(4), 57-70.

Balaam, N. P., & Booker, J. R. (1981). Analysis of rigid rafts supported by granular piles. International journal for numerical and analytical methods in geomechanics, 5(4), 379-403.

Barron, R. A. (1948). Consolidation of fine-grained soils by drain wells by drain wells. Transactions of the American Society of Civil Engineers, 113(1), 718-742.

Baumann, V., and G. E. A. Bauer. The performance of foundations on various soils stabilized by the vibro-compaction method. Canadian Geotechnical Journal 11, no. 4 (1974): 509-530.

Bjerrum, L. (1967). Engineering geology of Norwegian normally-consolidated marine clays as related to settlements of buildings. Geotechnique, 17(2), 83-118.

Chai, J. C., Miura, N., Kirekawa, T., & Hino, T. (2010). Settlement prediction for soft ground improved by columns. Proceedings of the Institution of Civil Engineers-Ground Improvement, 163(2), 109-119.

Chai, J., & Pongsivasathit, S. (2010). A method for predicting consolidation settlements of floating column improved clayey subsoil. Frontiers of Architecture and Civil engineering in China, 4(2), 241-251.

Chai, J. C., Shrestha, S., Hino, T., Ding, W. Q., Kamo, Y., & Carter, J. (2015). 2D and 3D analyses of an embankment on clay improved by soil–cement columns. Computers and Geotechnics, 68, 28-37.

Chen, R. P., Chen, Y. M., Han, J., & Xu, Z. Z. (2008). A theoretical solution for pile-supported embankments on soft soils under one-dimensional compression. Canadian Geotechnical Journal, 45(5), 611-623.

Chen, Z. J., Feng, W. Q., & Yin, J. H. (2021). A new simplified method for calculating short-term and long-term consolidation settlements of multi-layered soils considering creep limit. Computers and Geotechnics, 138, 104324.

Degago, S. A., Grimstad, G., Jostad, H. P., & Nordal, S. (2013). Misconceptions about experimental substantiation of creep hypothesis A. In Proceedings of the 18th International Conference on Soil Mechanics and Geotechnical Engineering, Paris (pp. 215-218).

Fang, Z., & Yin, J. H. (2007). Responses of excess pore water pressure in soft marine clay around a soil–cement column. International Journal of Geomechanics, 7(3), 167-175.

Feng, W. Q., & Yin, J. H. (2017). A new simplified Hypothesis B method for calculating consolidation settlements of double soil layers exhibiting creep. International Journal for Numerical and Analytical Methods in Geomechanics, 41(6), 899-917.

Feng, W. Q., & Yin, J. H. (2018). A new simplified Hypothesis B method for calculating the consolidation settlement of ground improved by vertical drains. International Journal for Numerical and Analytical Methods in Geomechanics, 42(2), 295-311.

Feng, W. Q., Yin, J. H., Chen, W. B., Tan, D. Y., & Wu, P. C. (2020a). A new simplified method for calculating consolidation settlement of multi-layer soft soils with creep under multi-stage ramp loading. Engineering Geology, 264, 105322.

Feng, W. Q., Tan, D. Y., Yin, J. H., Qin, J. Q., & Chen, W. B. (2020b). Experimental and numerical studies on the performances of stone column and sand compaction pile–reinforced Hong Kong marine clay. International Journal of Geomechanics, 20(8), 06020018.

Feng, W. Q., Yin, J. H., Chen, W. B., & Wu, P. C. (2021). Development and performance of new simplified method for soft soil with creep under multi-staged loading. Marine Georesources & Geotechnology, 39(4), 431-447.

Garlanger, J. E. (1972). The consolidation of soils exhibiting creep under constant effective stress. Geotechnique, 22(1), 71-78.

Han, J., & Ye, S. L. (2001). Simplified method for consolidation rate of stone column reinforced foundations. Journal of Geotechnical and Geoenvironmental Engineering, 127(7), 597-603.

Han, J., & Ye, S. L. (2002). A theoretical solution for consolidation rates of stone column-reinforced foundations accounting for smear and well resistance effects. International Journal of Geomechanics, 2(2), 135-151.

Hansbo, S. (1979). Consolidation of clay by bandshaped prefabricated drains. Ground Engineering, 12(5).

Horpibulsuk, S., Chinkulkijniwat, A., Cholphatsorn, A., Suebsuk, J., & Liu, M. D. (2012). Consolidation behavior of soil–cement column improved ground. Computers and Geotechnics, 43, 37-50.

Ho, T. O., Tsang, D. C., Chen, W. B., & Yin, J. H. (2020). Evaluating the environmental impact of contaminated sediment column stabilized by deep cement mixing. Chemosphere, 261, 127755.

Huang, J., & Han, J. (2009). 3D coupled mechanical and hydraulic modeling of a geosynthetic-reinforced deep mixed column-supported embankment. Geotextiles and Geomembranes, 27(4), 272-280.

Jiang, L., & Lin, H. (2010). Integrated analysis of SAR interferometric and geological data for investigating long-term reclamation settlement of Chek Lap Kok Airport, Hong Kong. Engineering Geology, 110(3-4), 77-92.

Legislative Council Panel on Economic Development. (2019) Update on the Development of the Three-Runway System at the Hong Kong International Airport https://www.legco.gov.hk/yr18-19/english/panels/edev/papers/edev20190429cb4-775-5-e.pdf

Liu, S., Zhang, D., Song, T., Zhang, G., & Fan, L. (2022). A Method of Settlement Calculation of Ground Improved by Floating Deep Mixed Columns Based on Laboratory Model Tests and Finite Element Analysis. International Journal of Civil Engineering, 20(2), 207-222.

Long, R. P., & Covo, A. (1994). Equivalent diameter of vertical drains with an oblong cross section. Journal of Geotechnical Engineering, 120(9), 1625-1630.

Lu, M., Li, D., Jing, H., & Deng, Y. (2019). Analytical solution for consolidation of band-shaped drain based on an equivalent annular drain. International Journal of Geomechanics, 19(6), 04019043.

Madhav, M., Suresh, K., & Peter, E. (2010). Effect of creep on settlement of granular pile reinforced ground. International Journal of Geotechnical Engineering, 4(4), 495-505.

Mesri, G. R. E. S., Febres-Cordero, E., Shields, D., & Castro, A. (1981). Shear stress-strain-time behaviour of clays. Geotechnique, 31(4), 537-552.

Pongsivasathit, S., Chai, J., & Ding, W. (2013). Consolidation settlement of floating-column-improved soft clayey deposit. Proceedings of the Institution of Civil Engineers-Ground Improvement, 166(1), 44-58.

Qin, J. Q., Feng, W. Q., Wu, P. C., & Yin, J. H. (2020). Fabrication and performance evaluation of a novel FBG-based effective stress cell for directly measuring effective stress in saturated soils. Measurement, 155, 107491.

Sexton, B. G., McCabe, B. A., Karstunen, M., & Sivasithamparam, N. (2016). Stone column settlement performance in structured anisotropic clays: the influence of creep. Journal of Rock Mechanics and Geotechnical Engineering, 8(5), 672-688.

Sexton, B. G., Sivakumar, V., & McCabe, B. A. (2017). Creep improvement factors for vibro-replacement design. Proceedings of the Institution of Civil Engineers-Ground Improvement, 170(1), 35-56.

Shahu, J. T., Madhav, M. R., & Hayashi, S. (2000). Analysis of soft ground-granular pile-granular mat system. Computers and Geotechnics, 27(1), 45-62.

Shepheard, C. J., & Williamson, M. G. (2018, November). Thoughts on a Simple Means of Estimating Settlement in Thick Soil Layers in Accordance with Hypothesis B. In International Congress and Exhibition" Sustainable Civil Infrastructures: Innovative Infrastructure Geotechnology" (pp. 54-63). Springer, Cham.

Sivakumar, V., Moorhead, M. C., Donohue, S., Serridge, C. J., Tripathy, S., Mckinley, J., & Doherty, C. (2021). The initial, primary and secondary consolidation response of soft clay reinforced with a granular column under isolated loading. Géotechnique, 71(6), 467-479.

Sloan, J., Filz, G.M., & Collin, J. (2011). A generalized formulation of the adapted terzaghi method of arching in column-supported embankments. In Geo-Frontiers 2011: Advances in Geotechnical Engineering (pp. 798-805).

Wu, P. C., Yin, J. H., Feng, W. Q., & Chen, W. B. (2019). Experimental study on geosynthetic-reinforced sand fill over marine clay with or without deep cement mixed soil columns under different loadings. Underground Space, 4(4), 340-347.

Wu, P. C., Feng, W. Q., & Yin, J. H. (2020). Numerical study of creep effects on settlements and load transfer mechanisms of soft soil improved by deep cement mixed soil columns under embankment load. Geotextiles and Geomembranes, 48(3), 331-348.

Yapage, N. N. S., Liyanapathirana, D. S., Kelly, R. B., Poulos, H. G., & Leo, C. J. (2014). Numerical modeling of an embankment over soft ground improved with deep cement mixed columns: case history. Journal of Geotechnical and Geoenvironmental Engineering, 140(11), 04014062.

Jian-hua, YIN. (2011). From constitutive modeling to development of laboratory testing and optical fiber sensor monitoring technologies. Chinese Journal of Geotechnical Engineering, 01.

Yin, J. H. (2015). Fundamental issues of elastic viscoplastic modeling of the time-dependent stress–strain behavior of geomaterials. International Journal of Geomechanics, 15(5), A4015002.

Yin, J. H., Chen, Z. J., & Feng, W. Q. (2022). A general simple method for calculating consolidation settlements of layered clayey soils with vertical drains under staged loadings. Acta Geotechnica, 1-28.

Yin, J. H., & Fang, Z. (2006). Physical modelling of consolidation behaviour of a composite foundation consisting of a cement-mixed soil column and untreated soft marine clay. Geotechnique, 56(1), 63-68.

Yin, J. H., & Fang, Z. (2010). Physical modeling of a footing on soft soil ground with deep cement mixed soil columns under vertical loading. Marine Georesources and Geotechnology, 28(2), 173-188.

Yin, J. H., & Feng, W. Q. (2017). A new simplified method and its verification for calculation of consolidation settlement of a clayey soil with creep. Canadian Geotechnical Journal, 54(3), 333-347.

Yin, J. H., & Graham, J. (1989). Viscous–elastic–plastic modelling of one-dimensional time-dependent behaviour of clays. Canadian geotechnical journal, 26(2), 199-209.

Yin, J. H., & Graham, J. (1994). Equivalent times and one-dimensional elastic viscoplastic modelling of time-dependent stress–strain behaviour of clays. Canadian Geotechnical Journal, 31(1), 42-52.

Yin, J. H., & Graham, J. (1996). Elastic visco-plastic modelling of one-dimensional consolidation. Geotechnique, 46(3), 515-527.

Yin, J. H., & Zhu, J. G. (1999). Elastic viscoplastic consolidation modelling and interpretation of pore-water pressure responses in clay underneath Tarsiut Island. Canadian Geotechnical Journal, 36(4), 708-717.

Yin, J. H., & Zhu, G. (2020). Consolidation Analyses of Soils. CRC Press.

Yin, Z. Y., Karstunen, M., & Hicher, P. Y. (2010). Evaluation of the influence of elasto-viscoplastic scaling functions on modelling time-dependent behaviour of natural clays. Soils and Foundations, 50(2), 203-214.

Yu, X. J., Fang, Z., Yin, J. H., Wang, S. Y., & Yan, Y. (2007). Numerical Modelling of Soft Soil Installed by PVDs. In Key Engineering Materials (Vol. 340, pp. 1249-1254). Trans Tech Publications Ltd.

Zaman, M., Gopalasingam, A., & Laguros, J. G. (1991). Consolidation settlement of bridge approach foundation. Journal of Geotechnical Engineering, 117(2), 219-240.

Zhao, L. S., Zhou, W. H., & Yuen, K. V. (2017). A simplified axisymmetric model for column supported embankment systems. Computers and Geotechnics, 92, 96-107.

Zhou, W. H., Lok, T. M. H., Zhao, L. S., Mei, G. X., & Li, X. B. (2017). Analytical solutions to the axisymmetric consolidation of a multi-layer soil system under surcharge combined with vacuum preloading. Geotextiles and Geomembranes, 45(5), 487-498.

Zhou, Y., Kong, G., Wen, L., & Yang, Q. (2021). Evaluation of geosynthetic-encased column-supported embankments with emphasis on penetration of column toe. Computers and Geotechnics, 132, 104039.

Zhu, G., & Yin, J. H. (2000). Elastic visco-plastic consolidation modelling of clay foundation at Berthierville test embankment. International journal for numerical and analytical methods in geomechanics, 24(5), 491-508.

Zhu, G., Yin, J. H., & Graham, J. (2001). Consolidation modelling of soils under the test embankment at Chek Lap Kok International Airport in Hong Kong using a simplified finite element method. Canadian Geotechnical Journal, 38(2), 349-363.

Zhu, G., & Yin, J. H. (2004). Consolidation analysis of soil with vertical and horizontal drainage under ramp loading considering smear effects. Geotextiles and Geomembranes, 22(1-2), 63-74.

Appendix

Example 1

Sublayer m = 3 in Stage III

$p = 11\,\text{kPa}$, $\text{POP} = 12\ \text{kPa}$, $C_c / v = 0.2348$, $C_s / v = 0.0297$, $C_{ae} / v = 0.0092$, $t_0 = 1$ day , $t = 500$ day ($U_a = 1$), $t_{EOP.field} \approx 90$ day .

(1). $\sigma'_{v0,3} = (16.5 - 9.8) \times 0.188 = 1.756$ kPa ;

(2). Treated by DCM soil columns,

$$A_r = 10.96\% ,$$

$$n_s = 3.92 ;$$

(3). Using Eq. (11):

$$\sigma'_s = 11 / (1 - 10.96\% + 3.29 \times 10.96\%) = 8.796 \text{ kPa} ;$$

(4). $\sigma'_{v1,3} = 1.756 + 8.796 = 10.552$ kPa $< \sigma'_{vp,3} = 1.756 + 12 = 13.756$ kPa → *O.C.*;

(5). Using Eq. (7):

$$\varepsilon_{f,3} = 0.0297 \times \log(10.552 / 1.756) = 0.023 ;$$

(6). Using Eq. (12):

$$\varepsilon_{creep,f,3} = (1 - 10.96\%)^1 \times 0.0092 \times \log\left(\frac{500 + 368.48}{1 + 368.48}\right) = 0.00304 ,$$

Using Eq.16 $\Delta t_{e,3} = 368.48$ day ;

(7). Using Eq. (14)

$$\varepsilon_{creep,d,3} = (1 - 10.96\%)^1 \times 0.0092 \times \log\left(\frac{500 + 368.48}{90 + 368.48}\right) = 0.02409 ;$$

(8). $\varepsilon_{creep,3} = U_a \varepsilon_{creep,f,3} + (1 - U_a) \varepsilon_{creep,d,3} = 0.00304$;

(9). $\varepsilon_{v1,f1,3} = \varepsilon_{f,3} + \varepsilon_{creep,3} + \varepsilon_{v0,f0,3} = 0.026$.

Example 2

Sublayer m = 2 in Stage I

$p = 12$ kPa , $\mathrm{POP} = 4$ kPa , $C_c / v = 0.2348$, $C_s / v = 0.0297$, $C_{ae} / v = 0.0092$, $t_0 = 1$ day , $t = 83$ day ($U_a = 1$), $t_{EOP.field} \approx 20$ day .

(1). $\sigma'_{v0,2} = (16.5 - 9.8) \times 0.143 = 1.460$ kPa ;

(2). Treated by PVDs,

$$A_r = 1.11\%,$$

$$n_s = 1;$$

(3). Using Eq. (11):

$$\sigma'_s = 12 / (1 - 1.11\% + 1 \times 1.11\%) = 12 \text{ kPa};$$

(4). $\sigma'_{v1,2} = 1.460 + 12 = 13.460 \text{ kPa} > \sigma'_{vp,2} = 1.460 + 4 = 5.460 \text{ kPa} \rightarrow$ *N.C.*;

(5). Using Eq. (8):

$$\varepsilon_{f,2} = 0.0297 \times \log(5.460 / 1.460) + 0.2348 \times \log(13.460 / 5.460) = 0.109;$$

(6). Using Eq. (13):

$$\varepsilon_{creep,f,2} = (1 - 1.11\%)^1 \times 0.0092 \times \log(83/1) = 0.01746;$$

(7). Using Eq. (15):

$$\varepsilon_{creep,d,2} = (1 - 1.11\%)^1 \times 0.0092 \times \log(83/20) = 0.00562;$$

(8). $\varepsilon_{creep,2} = U_a \varepsilon_{creep,f,2} + (1 - U_a) \varepsilon_{creep,d,2} = 0.01746$;

(9). $\varepsilon_{v1,f1,2} = \varepsilon_{f,2} + \varepsilon_{creep,2} + \varepsilon_{v0,f0,2} = 0.126$.

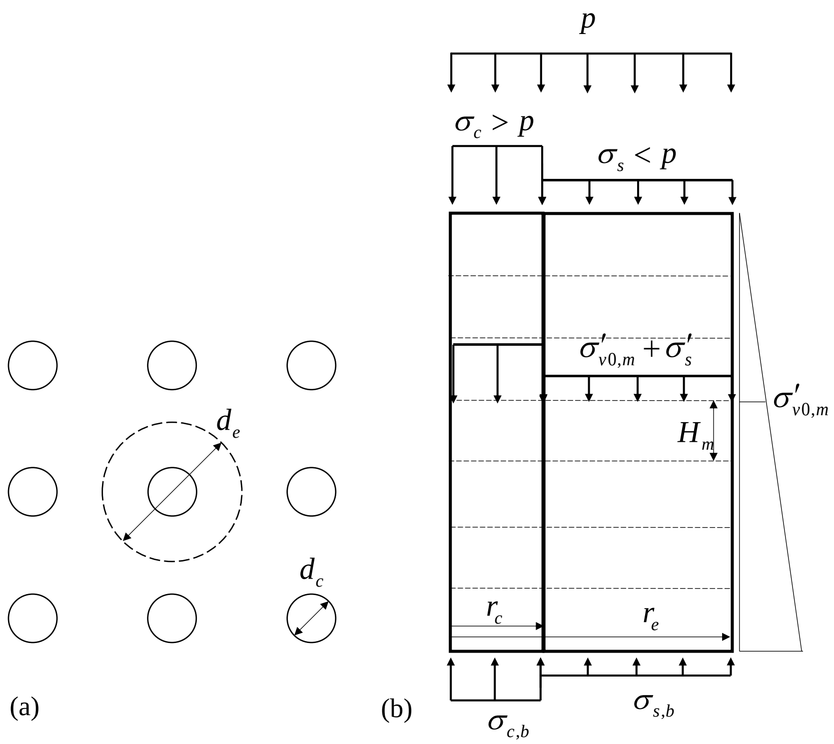

Figure 1. Schematic diagram of (a) the unit cell and (b) the loading distribution between column and its surrounding soils

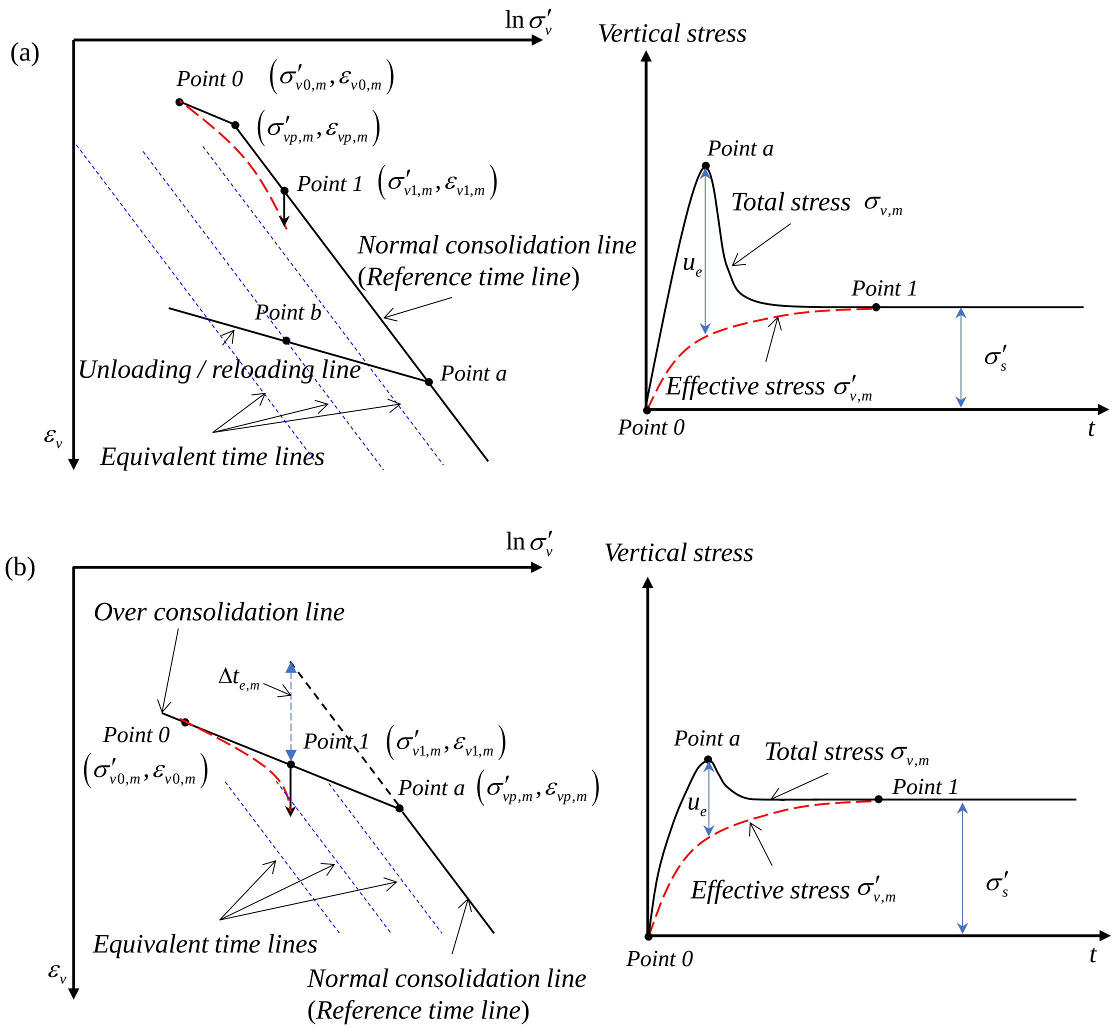

817

818 Figure 2. Illustration of stress-strain relationships of surrounding soils for (a) normally
819 consolidated state and (b) over-consolidated state in column treated soft soil ground

820

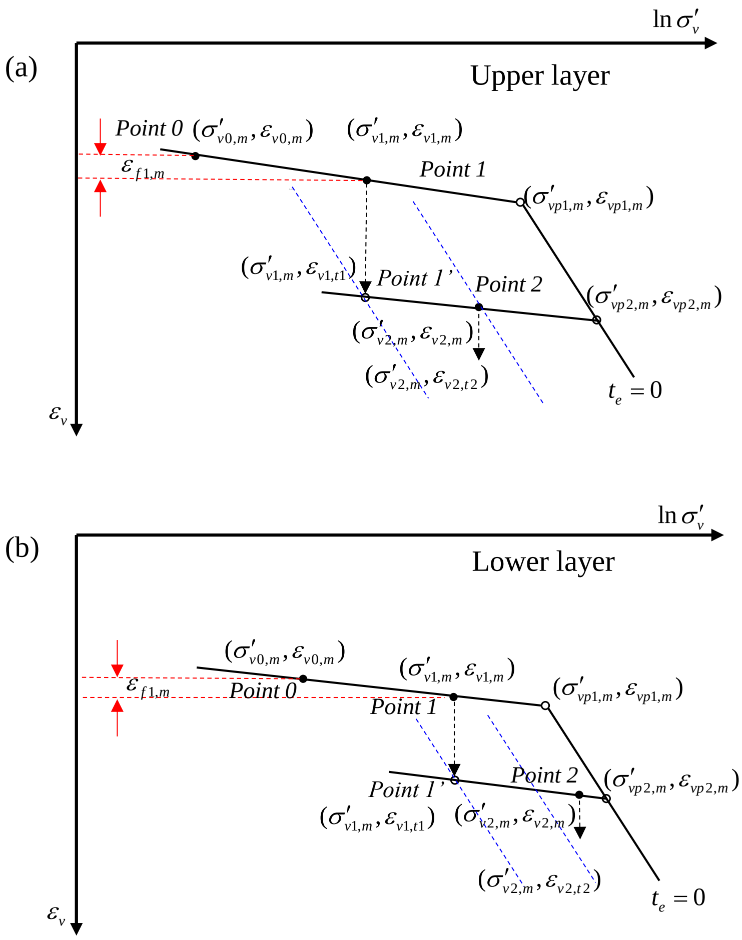

Figure 3. Schematic diagram of stress-strain paths in a double-layer soft soil under two-staged loading: (a) upper layer and (b) lower layer

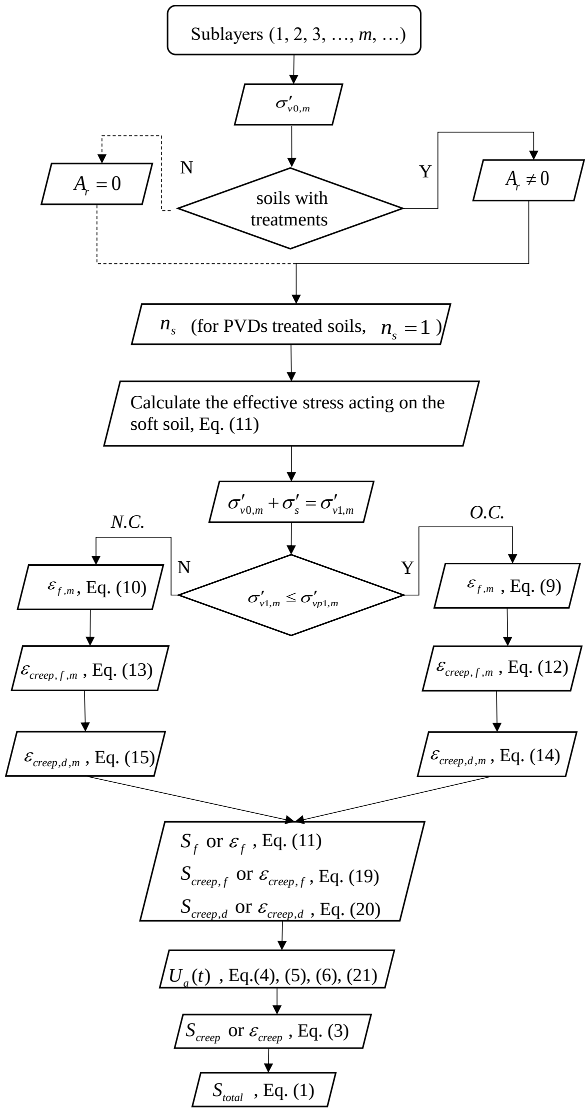

Figure 4. Calculation flow chart of the simple calculation method

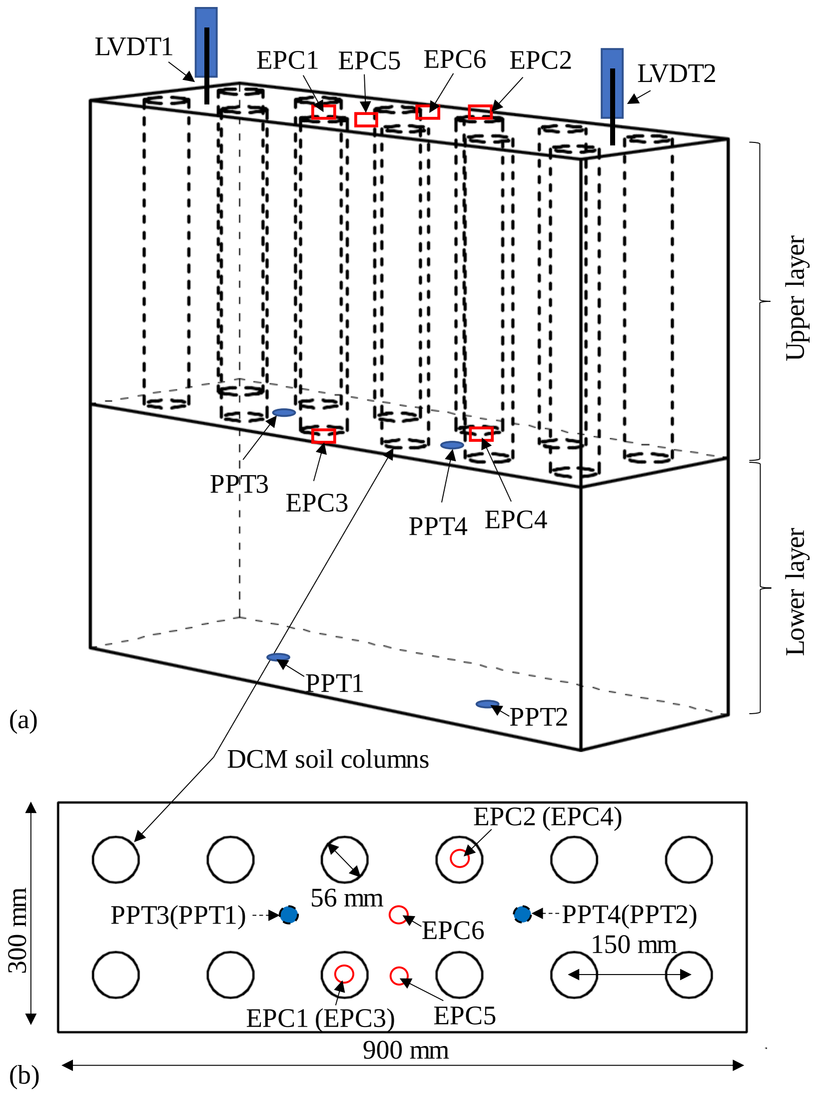

Figure 5. Physical model test with DCM soil columns and layout of transducers: (a) side view and (b) top view

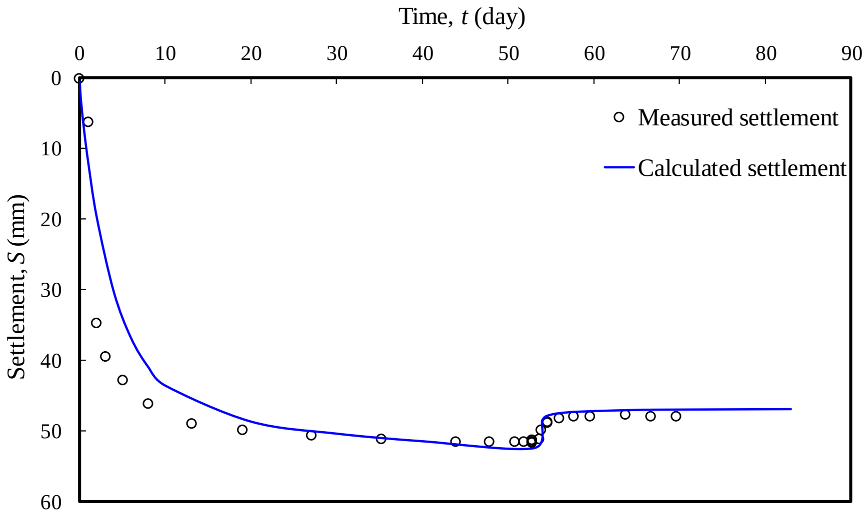

834

835 Figure 6. The comparison of measured settlement and calculated settlement for the double-
836 layer soft soil improved by PVDs under loading and unloading processes

837

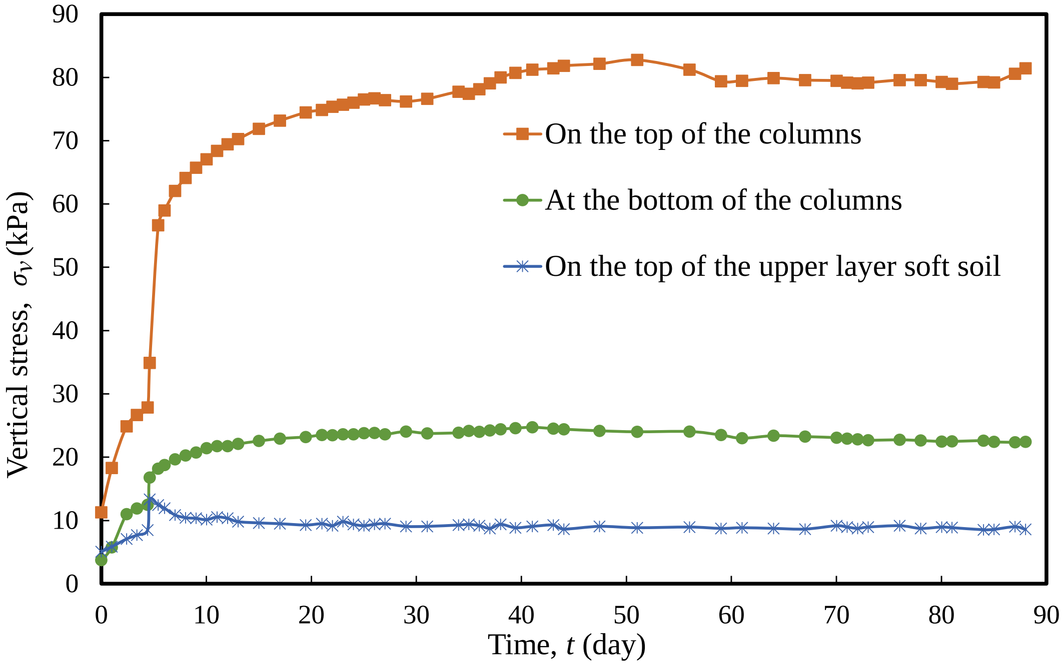

Figure 7. Measured vertical stresses in the upper layer of the soft soil improved by DCM soil columns

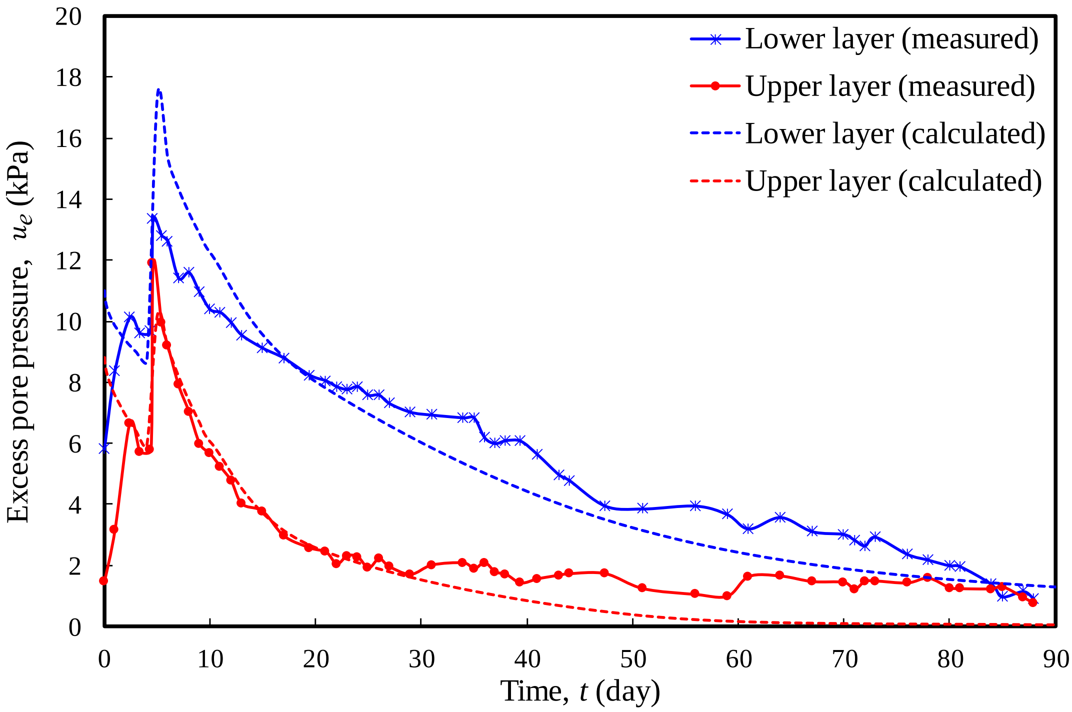

Figure 8. The comparison of measured and calculated excess pore pressures in the double-layer soft soil improved by DCM soil columns

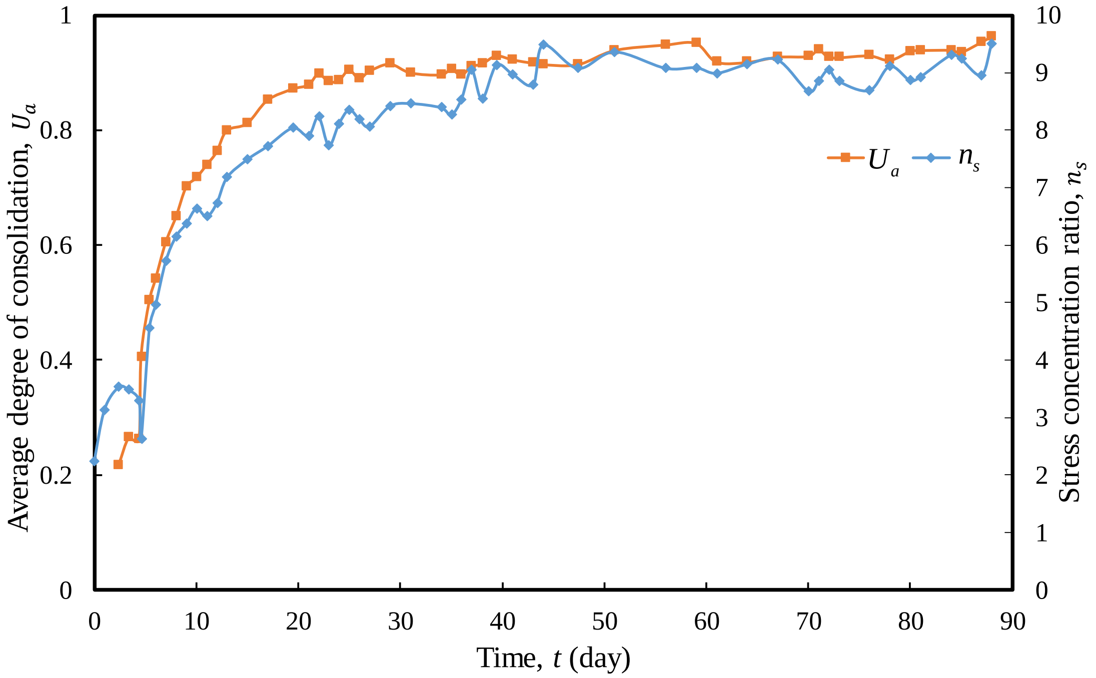

Figure 9. The curves of average degree of consolidation and stress concentration ratio *versus* time

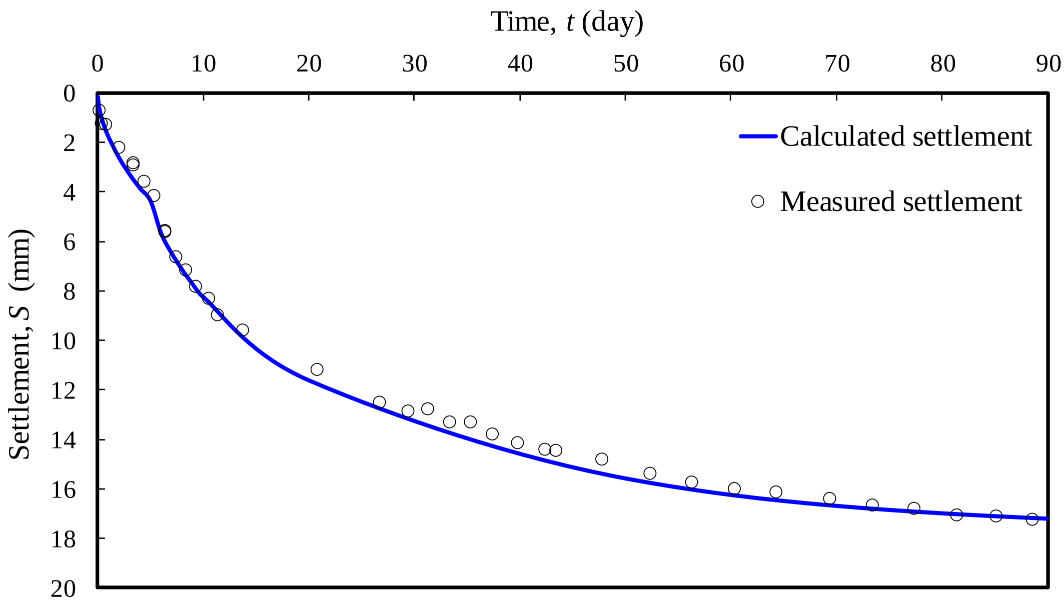

Figure 10. The comparison of measured settlement and calculated settlement for the double-layer soft soil improved by DCM soil columns

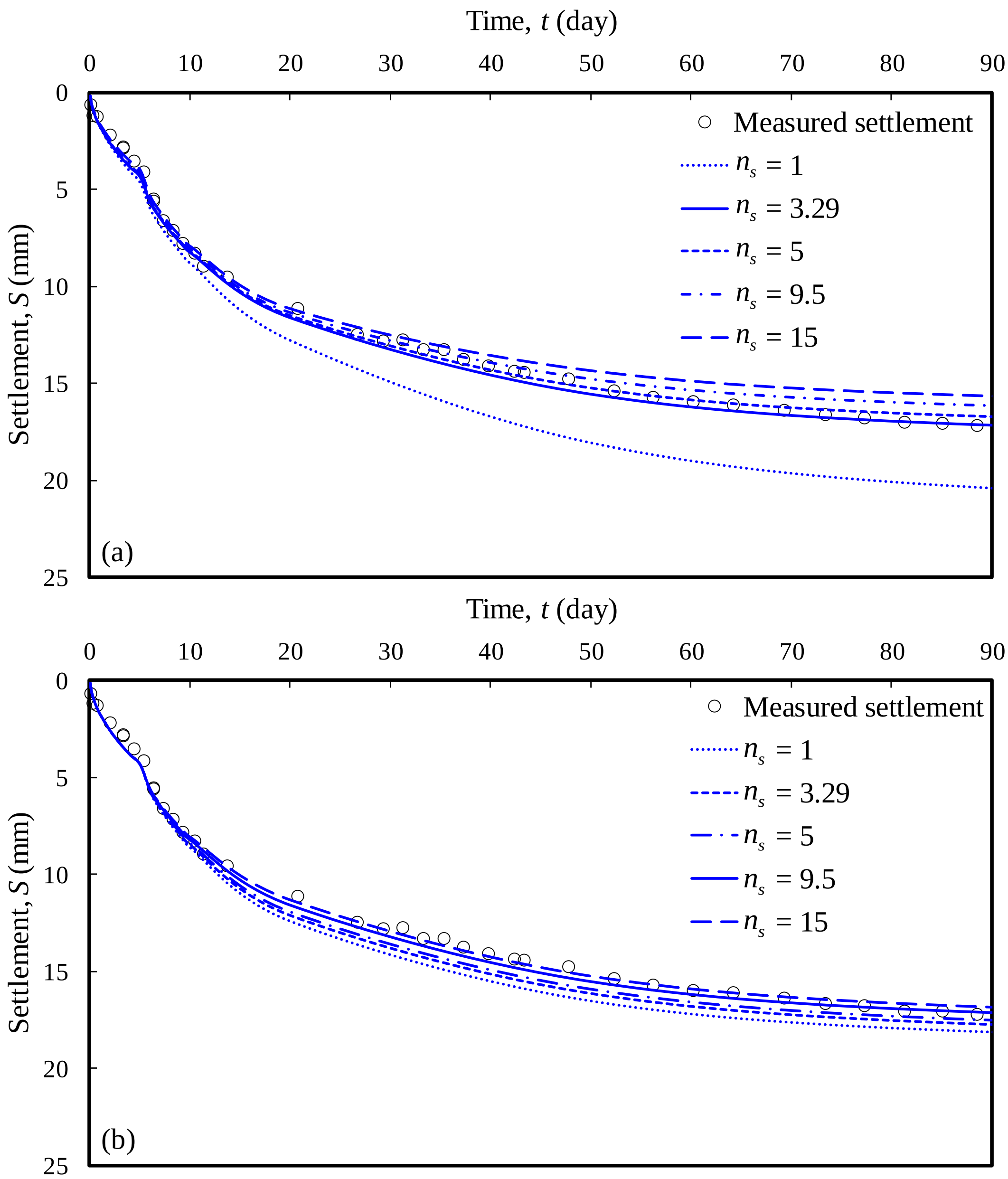

855

856 Figure 11. Influence of the stress concentration ratio n_s on settlement (a) for 11 kPa loading
857 in Stage III and (b) for 20 kPa loading in Stage III

858

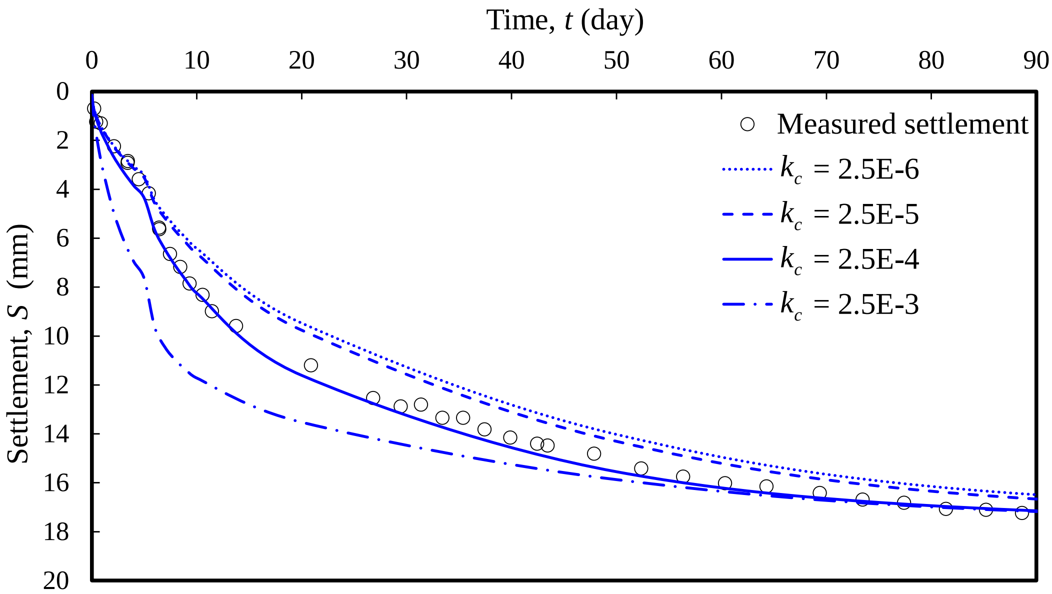

Figure 12. Influence of coefficient of permeability of DCM soil columns k_c

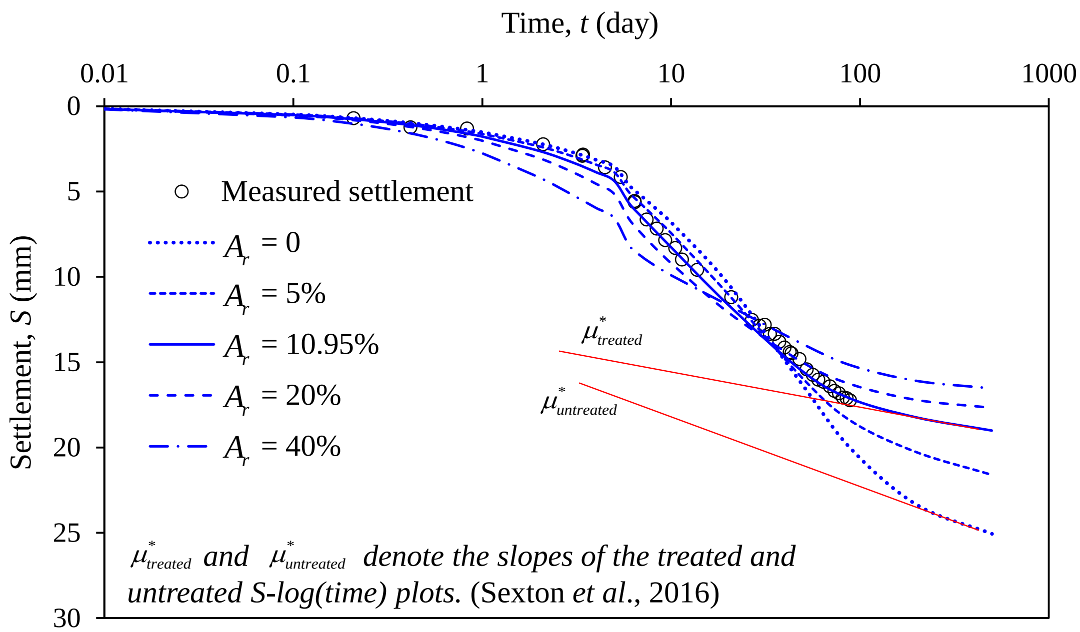

Figure 13. Influence of area replacement ratio A_r on settlement

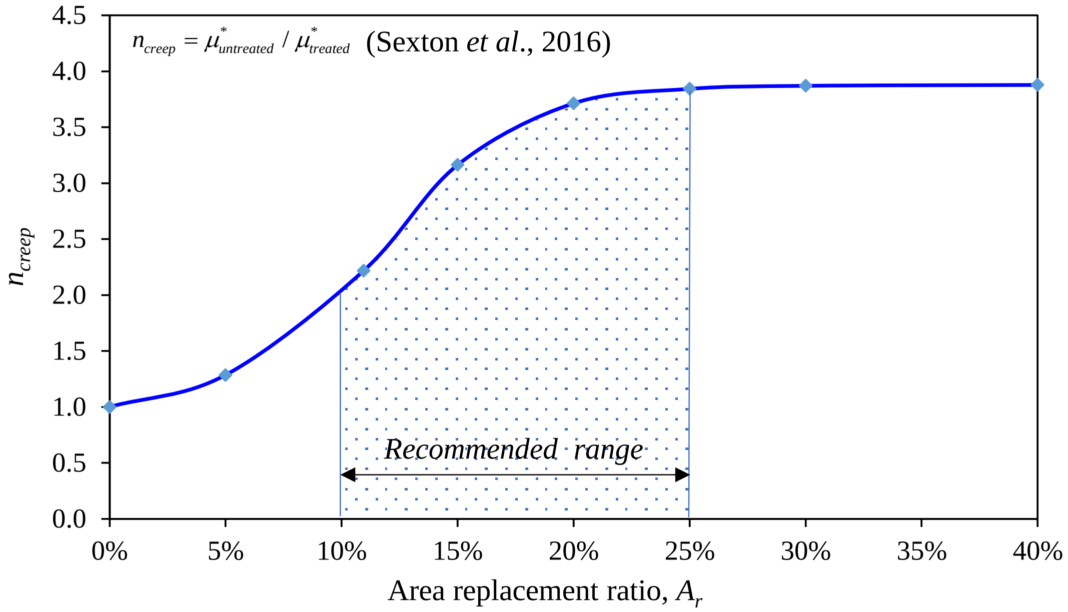

Figure 14. Influence of area replacement ratio A_r on creep settlement improvement factor

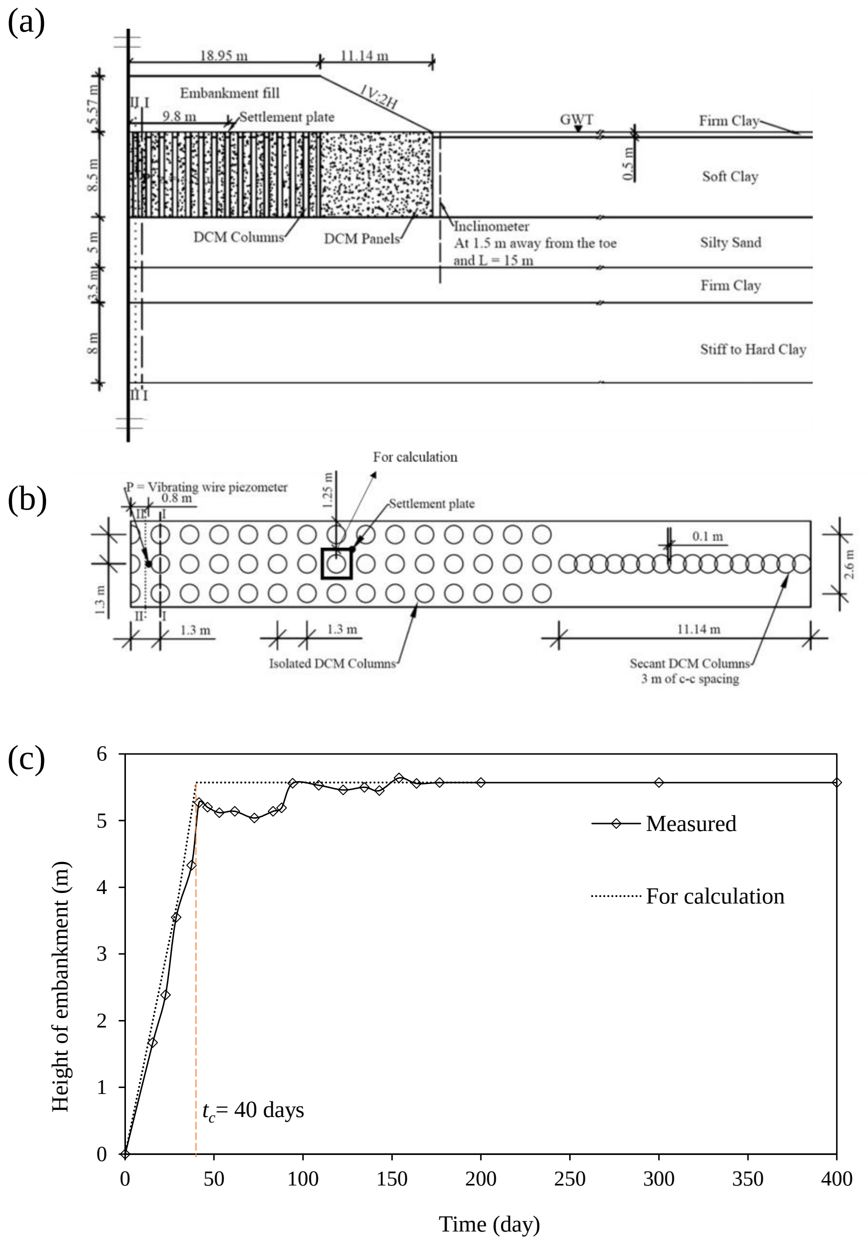

Figure 15. (a) Geometries of the embankment over a soft soil improved by DCM columns; (b) layout of DCM columns and (c) Construction duration of the embankment (after Yapage *et al.*, 2014)

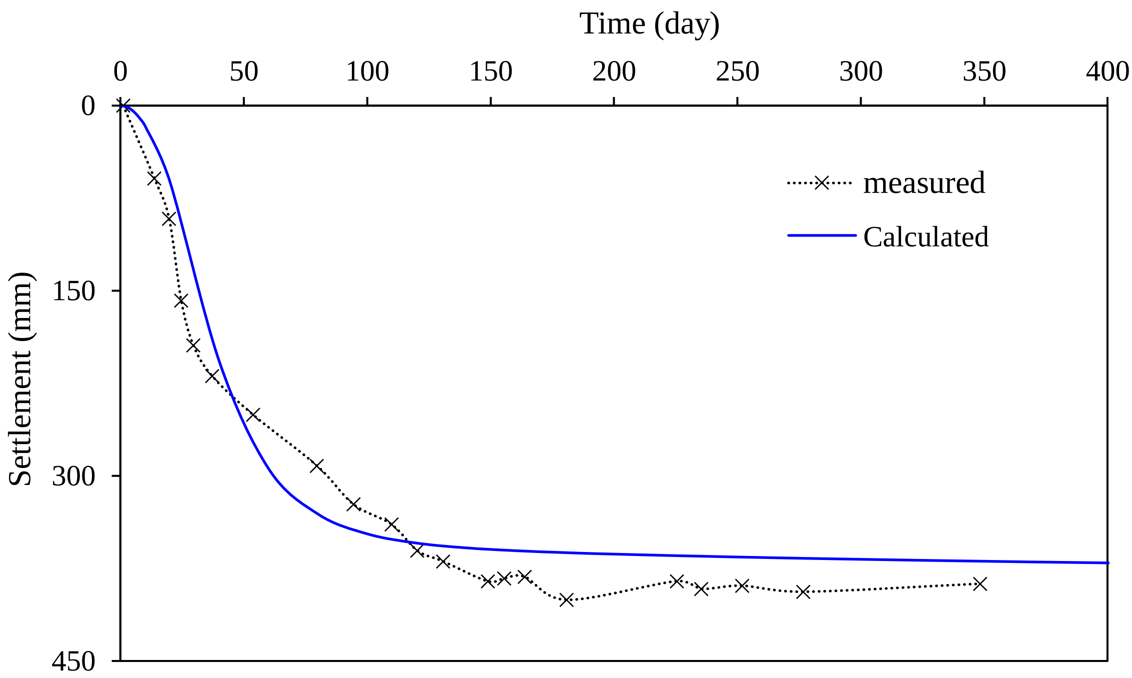

Figure 16. Comparison between the measured settlement and the settlement calculated by proposed simple method with different value of stress concentration ratio

Table 1. Basic properties of the reconstituted Hong Kong marine deposits

G_s	*LL* (%)	*PL* (%)	*PI* (%)	PSD Clay (%)	PSD Silt (%)	PSD Sand and Gravel (%)
2.65	43.20	22.60	20.60	11.41	66.80	21.79

Note: G_s is the specific gravity, *LL* is the liquid limit, *PL* is the plastic limit, *PI* is the plasticity Index, PSD is the particle size distribution.

Table 2. Basic properties of DCM soil columns

ρ_d (kg/m^3)	w (%)	c/s (%)	d_c (mm)	L (mm)	k_c (m/day)
900	100	20	56	300	2.5E-4

Note: *c/s* is the cement/soil ratio.

Table 3. Properties of the reconstituted HKMD used for calculation (Stage I and II)

Layer	γ (kN/m^3)	C_c / v	C_s / v	C_{ae} / v	k_r (m/day)	k_v (m/day)	POP (kPa)
Upper	16.5	0.2348	0.0297	0.0092	1.12E-4	5.61E-5	4
Lower	16.5	0.2666	0.0326	0.0050	5.12E-5	2.56E-5	15

Note: POP is the pressure of pre-consolidation.

Table 4. Properties of the reconstituted HKMD used for calculation (Stage III)

Layer	γ (kN/m^3)	C_c / v	C_s / v	C_{ae} / v	k_r (m/day)	k_v (m/day)	POP (kPa)
Upper	16.5	0.2348	0.0297	0.0092	3.64E-5	1.82E-5	12
Lower	16.5	0.2666	0.0326	0.0050	3.04E-5	1.52E-5	15

Note: POP is the pressure of pre-consolidation.

Table 5. Calculation procedure of the double layered soft soil improved by DCM soil columns

Stage III 11kPa

m	Middle depth (m)	$\sigma'_{v0,m}$ (kPa)	$\sigma'_{vp1,m}$ (kPa)	$\sigma'_{v1,m}$ (kPa)	$\varepsilon_{vp1,m}$	$\varepsilon_{f1,m}$	$\varepsilon_{v1,m}$	$\varepsilon_{v1,t1,m}-\varepsilon_{v0,t0,m}$	$\varepsilon_{v1,t1}$	$\Delta t_{e1,m}$ (day)	m_v (kPa^{-1})
1	0.038	0.751	12.751	9.547	0.037	0.033	0.033	0.035	0.035	633.068	
2	0.113	1.254	13.254	10.050	0.030	0.027	0.027	0.029	0.029	477.306	2.93E-3
3*	0.188	1.756	13.756	10.552	0.027	0.023	0.023	0.026	0.026	368.476	
4	0.263	2.259	14.259	11.055	0.024	0.020	0.020	0.024	0.024	290.421	
5	0.352	2.856	17.856	13.856	0.026	0.022	0.022	0.025	0.025	262.491	
6	0.455	3.549	18.549	14.549	0.023	0.020	0.020	0.023	0.023	207.194	1.83E-3
7	0.558	4.241	19.241	15.241	0.021	0.018	0.018	0.021	0.021	166.689	

Stage III 20 kPa

m	Middle depth (m)	$\sigma'_{v1,m}$ (kPa)	$\sigma'_{vp1,m}$ (kPa)	$\sigma'_{vp2,m}$ (kPa)	$\sigma'_{v2,m}$ (kPa)	$\varepsilon_{vp1,m}$	$\varepsilon_{vp2,m}$	$\varepsilon_{f2,m}$	$\varepsilon_{v2,m}$	$\varepsilon_{v1,t1}$	$\varepsilon_{v2,t2,m}-\varepsilon_{v1,t1,m}$	$\varepsilon_{v2,t2}$	$\Delta t_{e2,m}$ (day)	m_v (kPa^{-1})
1	0.038	9.547	12.751	25.077	14.211	0.037	0.045	0.005	0.040	0.035	0.005	0.040	1.29E+12	
2	0.113	10.050	13.254	26.597	14.713	0.030	0.039	0.005	0.034	0.029	0.005	0.034	5.04E+12	1.03E-3
3	0.188	10.552	13.756	28.155	15.216	0.027	0.036	0.005	0.031	0.026	0.005	0.031	1.92E+13	
4	0.263	11.055	14.259	29.749	15.718	0.024	0.033	0.005	0.029	0.024	0.005	0.029	7.08E+13	
5	0.352	13.856	17.856	38.029	22.856	0.026	0.029	0.007	0.032	0.025	0.007	0.032	1.82E+12	
6	0.455	14.549	18.549	40.181	23.549	0.023	0.027	0.007	0.029	0.023	0.007	0.029	8.23E+12	7.59E-4
7	0.558	15.241	19.241	42.368	24.241	0.021	0.025	0.007	0.028	0.021	0.007	0.028	3.47E+13	

Notes: * Example 1 in the **Appendix.**

Table 6. Calculation procedure of the double layered soft soil improved by PVDs

Stage I Loading

m	Middle depth (m)	$\sigma'_{v0,m}$ (kPa)	$\sigma'_{vp1,m}$ (kPa)	$\sigma'_{v1,m}$ (kPa)	$\varepsilon_{vp1,m}$	$\varepsilon_{f1,m}$	$\varepsilon_{v1,m}$	$\varepsilon_{v1,t1,m}-\varepsilon_{v0,t0,m}$	$\varepsilon_{v1,t1}$	$\Delta t_{e1,m}$ (day)	m_v (kPa^{-1})
1	0.048	0.820	4.820	12.820	0.023	0.123	0.123	0.140	0.140	0.00	8.80E-3
2*	0.143	1.460	5.460	13.460	0.017	0.109	0.109	0.126	0.126	0.00	
3	0.239	2.100	6.100	14.100	0.014	0.099	0.099	0.117	0.117	0.00	
4	0.334	2.739	6.739	14.739	0.012	0.091	0.091	0.109	0.109	0.00	
5	0.436	3.421	18.421	15.421	0.024	0.021	0.021	0.023	0.023	48.74	1.62E-3
6	0.544	4.145	19.145	16.145	0.022	0.019	0.019	0.021	0.021	41.34	
7	0.652	4.868	19.868	16.868	0.020	0.018	0.018	0.019	0.019	35.51	

Stage II Unloading

m	Middle depth (m)	$\sigma'_{v1,m}$ (kPa)	$\sigma'_{vp1,m}$ (kPa)	$\sigma'_{vp2,m}$ (kPa)	$\sigma'_{v2,m}$ (kPa)	$\varepsilon_{vp1,m}$	$\varepsilon_{vp2,m}$	$\varepsilon_{f2,m}$	$\varepsilon_{v2,m}$	$\varepsilon_{v1,t1}$	$\varepsilon_{v2,t2,m}-\varepsilon_{v1,t1,m}$	$\varepsilon_{v2,t2}$	$\Delta t_{e2,m}$ (day)	m_v kPa^{-1})
1	0.048	12.820	4.820	32.637	4.820	0.023	0.048	-0.013	0.127	0.140	-0.013	0.127	2.15E+60	1.41E-3
2	0.143	13.460	5.460	34.752	5.460	0.017	0.041	-0.012	0.115	0.126	0.000	0.126	5.07E+57	
3	0.239	14.100	6.100	36.897	6.100	0.014	0.037	-0.011	0.106	0.117	0.000	0.117	3.22E+55	
4	0.334	14.739	6.739	39.070	6.739	0.012	0.034	-0.010	0.099	0.109	0.000	0.109	4.41E+53	
5	0.436	15.421	18.421	40.023	7.421	0.024	0.011	-0.010	0.012	0.023	-0.009	0.014	2.07E+39	1.22E-3
6	0.544	16.145	19.145	42.250	8.145	0.022	0.010	-0.010	0.011	0.021	-0.008	0.013	2.96E+38	
7	0.652	16.868	19.868	44.504	8.868	0.020	0.008	-0.009	0.010	0.019	-0.007	0.012	5.71E+37	

Notes: * Example 2 in the **Appendix.**

Table 7. Properties of materials (after Yapage *et al.*, 2014)

Parameter	Top firm clay	Soft clay	Silty sand	Firm clay	Stiff clay	Fills	DCM
γ (kN/m^3)	18	14.5	18	16.5	16.5	19	18
e_0	2	3	2.23	2	2		
C_c	1.15	1.15					
C_s	0.06	0.06					
$C_{\alpha e}$	0.0236	0.0236					
E (MPa)			15	9	17	15	27.1
c' (kPa)	0.1	0.1	0.1	0.1	0.1		57.5
φ' (°)	25	25	30	25	25	30	27
k_v (m/day)	7.86×10^{-3}	5.18×10^{-3}	7.17×10^{-2}	5.18×10^{-5}	4.58×10^{-5}		5.18×10^{-3}
OCR	135	Depends on depth					